

## NRC Publications Archive Archives des publications du CNRC

### **Advancing synthetic fuel technology: a model study for the integration of direct air carbon capture and diesel synthesis**

Guzman-Urbina, Alexander; Thanapan, Tantiwatthanaphanich; Joy, Jubil; Anaya, Karina; Shadbahr, Jalil; Kumar, Amit; Gonzales-Calienes, Giovanna; Morimoto, Shinichirou

This publication could be one of several versions: author's original, accepted manuscript or the publisher's version. / La version de cette publication peut être l'une des suivantes : la version prépublication de l'auteur, la version acceptée du manuscrit ou la version de l'éditeur.

For the publisher's version, please access the DOI link below. / Pour consulter la version de l'éditeur, utilisez le lien DOI ci-dessous.

#### **Publisher's version / Version de l'éditeur:**

<https://doi.org/10.1016/j.jcou.2026.103319>

*Journal of CO2 Utilization*, 104, C, pp. 1-18, 2026-01-10

#### **NRC Publications Archive Record / Notice des Archives des publications du CNRC :**

<https://nrc-publications.canada.ca/eng/view/object/?id=c4498344-dd01-44f2-b277-6cbfcb7dcfd>

<https://publications-cnrc.canada.ca/fra/voir/objet/?id=c4498344-dd01-44f2-b277-6cbfcb7dcfd>

Access and use of this website and the material on it are subject to the Terms and Conditions set forth at

<https://nrc-publications.canada.ca/eng/copyright>

READ THESE TERMS AND CONDITIONS CAREFULLY BEFORE USING THIS WEBSITE.

L'accès à ce site Web et l'utilisation de son contenu sont assujettis aux conditions présentées dans le site

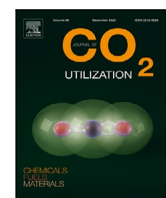
<https://publications-cnrc.canada.ca/fra/droits>

LISEZ CES CONDITIONS ATTENTIVEMENT AVANT D'UTILISER CE SITE WEB.








**Questions?** Contact the NRC Publications Archive team at

PublicationsArchive-ArchivesPublications@nrc-cnrc.gc.ca. If you wish to email the authors directly, please see the first page of the publication for their contact information.

**Vous avez des questions?** Nous pouvons vous aider. Pour communiquer directement avec un auteur, consultez la première page de la revue dans laquelle son article a été publié afin de trouver ses coordonnées. Si vous n'arrivez pas à les repérer, communiquez avec nous à PublicationsArchive-ArchivesPublications@nrc-cnrc.gc.ca.



## Advancing synthetic fuel technology: A model study for the integration of direct air carbon capture and diesel synthesis

Alexander Guzman-Urbina <sup>a</sup> <sup>\*</sup>, Tantiwatthanaphanich Thanapan <sup>a</sup> , Jubil Joy <sup>b</sup>,  
Karina Anaya <sup>b</sup> , Jalil Shadbahr <sup>c</sup> , Amit Kumar <sup>b</sup> , Giovanna Gonzales-Calienes <sup>c</sup> ,  
Shinichirou Morimoto <sup>a</sup> 

<sup>a</sup> National Institute of Advanced Industrial Science and Technology, Onogawa16-1, Tsukuba, 305-8569, Ibaraki, Japan

<sup>b</sup> University of Alberta, 116 St. and 85 Ave., Edmonton, T6G2R3, Alberta, Canada

<sup>c</sup> Clean Energy Innovation (CEI) Research Centre, National Research Council, 1200 Montreal Road, Ottawa, K1A 0R6, ON, Canada

### ARTICLE INFO

#### Keywords:

CO<sub>2</sub> utilization  
CO<sub>2</sub> removal  
Direct air capture  
Diesel  
Emission assessment

### ABSTRACT

Direct air capture (DAC) integrated with solid oxide electrolysis (SOEC) and Fischer–Tropsch (FT) synthesis is a promising way to produce carbon-neutral liquid fuels. However, the high demand for renewable electricity, particularly from electrolytic hydrogen production, and limited cross-process integration pose key challenges to this mode of production. This study addressed these constraints by modeling a fully integrated DAC–SOEC–FT diesel system using a commercial, equation-oriented simulation platform under steady-state conditions and assuming that renewable power supplied the SOEC unit. The process design incorporated thermal and process-level integration with waste heat from the calciner, FT reactor, and SOEC burner repurposed for internal heating and feed conditioning. System-derived byproducts (e.g., naphtha, purge gases) were used as internal fuels to minimize external energy inputs and avoid additional emissions. Results showed that under ideal thermal integration scenarios, the theoretical internal recovery of up to 78% of total process heat could substantially reduce reliance on external utilities. While SOEC remained the primary electricity consumer (29.8 MWh/t-diesel), internal energy recovery mitigated auxiliary demands. Cradle-to-gate CO<sub>2</sub> emissions were net-negative and reached  $-1.20$  kg-CO<sub>2</sub>/kg-diesel in Japan and  $-1.56$  kg-CO<sub>2</sub>/kg-diesel in Canada. These results emphasized the strong synergies unlocked by integrated system design and offered a pathway toward energy-efficient, carbon-negative synthetic diesel suited for hard-to-abate transport sectors.

### 1. Introduction

The imperative to reduce global greenhouse gas (GHG) emissions by 2050 has intensified in light of increasing climate-related impacts, including rising sea levels, more frequent extreme weather events, and biodiversity loss, many of which have been linked, with varying levels of confidence, to anthropogenic carbon dioxide (CO<sub>2</sub>) emissions [1,2]. These emissions are the primary driver of global warming, which poses severe risks to natural systems, human health, and global socioeconomic stability.

In recognition of this challenge, the international community adopted the Paris Agreement, which was a commitment to limit the increase of the global average temperature to well below 2 °C above pre-industrial levels and to pursue efforts to restrict the rise to 1.5 °C [3]. Achieving these climate goals demands a rapid and systemic transformation of the global energy system, including the industrial and

transportation sectors, through the widespread deployment of low-carbon technologies, renewable energy systems, and sustainable energy carriers [4,5]. The development and integration of carbon capture, utilization, and storage (CCUS) strategies, in particular, have been increasingly recognized as essential components of any pathway to deep decarbonization.

While direct electrification using renewable electricity is widely recognized as the most energy-efficient and cost-effective strategy for decarbonizing large portions of the global economy, its applicability has been constrained in so-called “hard-to-abate” sectors [6–8]. These sectors include long-distance, heavy-duty transportation, such as commercial aviation, maritime shipping, and long-haul trucking, as well as energy-intensive industrial processes that rely on high-temperature heat and involve inherent chemical transformations. Key examples include the production of iron and steel, ammonia, cement,

\* Corresponding author.

E-mail address: [alex.guzmanurbina@aist.go.jp](mailto:alex.guzmanurbina@aist.go.jp) (A. Guzman-Urbina).

### Nomenclature

AWE	Alkaline Water Electrolysis
BECCS	Bioenergy with Carbon Capture and Storage
CCU	Carbon Capture and Utilization
CDR	Carbon Dioxide Removal
DAC	Direct Air Capture
FTS	Fischer–Tropsch Synthesis
PEM	Proton Exchange Membrane Electrolysis
PSA	Pressure Swing Adsorption
RWGS	Reverse Water-Gas Shift Reaction
SOEC	Solid Oxide Electrolysis Cells

and petrochemicals, where electrification alone may not be technically or economically viable in the near term.

In these domains, the requirements for high energy density, operational reliability, and compatibility with existing infrastructure render full electrification technically challenging and economically unfeasible in the short to medium term. Accordingly, sustainable fuels, such as biofuels and synthetic fuels derived from captured CO<sub>2</sub> and renewable hydrogen (commonly referred to as electrofuels or e-fuels), have emerged as a critical near-term decarbonization strategy [9–12].

A primary advantage of sustainable fuels lies in their infrastructure compatibility: they can be blended with or substituted for conventional fossil fuels within existing distribution, storage, and combustion systems with minimal modification. Because this drop-in capability significantly lowers the barriers to adoption and enables more rapid market deployment, use of sustainable fuels can bridge the transition period while more transformative solutions, such as full electrification and hydrogen-based systems, continue to mature and scale [13,14].

Although the market for sustainable hydrocarbon fuels remains in its early stages, two main technological pathways are under development: (1) biofuels — such as biodiesel, bioethanol, biobutanol, biohydrogen, and biomethane — produced from biomass resources; and (2) green hydrogen-based synthetic hydrocarbons (e-fuels), including e-methanol, e-diesel, and e-kerosene, synthesized from renewable hydrogen and captured carbon dioxide. These fuels not only contribute to a circular carbon economy but also reduce lifecycle CO<sub>2</sub> emissions when sustainably sourced. However, both production pathways currently face considerable cost barriers compared to conventional fossil fuels [15,16].

While several studies have evaluated the techno-economic and environmental performance of synthetic fuels, especially e-methanol and e-kerosene, fewer works have focused on the integration of Direct Air Capture (DAC) with downstream hydrocarbon synthesis and internal energy recovery. On the assumption that sustainable fuels will play a pivotal role in decarbonizing hard-to-abate sectors, this article narrows its focus to the production of synthetic diesel (e-diesel) as a viable drop-in fuel for long-range transportation applications [11]. Because e-diesel, fuels synthesized from green hydrogen and captured CO<sub>2</sub>, offer high energy density and full compatibility with existing diesel engines and fueling infrastructure, it is an attractive option for near-term deployment in sectors such as maritime shipping, heavy-duty trucking, and remote industrial operations [9,15].

In particular, this study proposes a process integration model that couples a liquid sorbent-based Direct Air Carbon Capture (DAC) system with downstream e-diesel synthesis. Although still at the developmental stage, liquid-based DAC technologies offer several advantages, including lower energy requirements for regeneration, continuous operation, and enhanced compatibility with renewable energy systems [17–19]. Because the goal of the proposed system was to capture atmospheric CO<sub>2</sub> and convert it into synthetic diesel via renewable hydrogen,

the proposed system could establish a closed carbon loop that would advance both climate mitigation and energy security objectives [13].

The novelty of this work lies in the thermochemical integration of the DAC and e-diesel subsystems. Specifically, the modeling framework considered the re-utilization of hydrocarbon-rich byproduct gases from the Fischer–Tropsch (FT) synthesis process, such as tail gas and unconverted intermediates, as a combustion fuel for the oxy-fired calciner in the DAC loop. This internal energy recovery strategy reduces external fuel input requirements and supports process-level energy self-sufficiency. The model quantified the energy demands, carbon balances, and potential system-level synergies under various process conditions, with the overarching goal of evaluating the technical and environmental feasibility of integrated, near-zero synthetic diesel production pathways.

## 2. Background on carbon removal and synthetic fuel technologies

To contextualize the proposed DAC–SOEC–FT system, this section presents a concise review of relevant background topics. It begins with an overview of CO<sub>2</sub> emissions by end-use sector and introduces carbon dioxide removal strategies, with a focus on DAC as a viable pathway. Key enabling technologies, including electrolysis systems, CO<sub>2</sub> recovery processes, and FT synthesis, drawing on recent literature to assess their maturity, operational characteristics, and suitability for integration. Finally, it summarizes the life cycle emissions context for synthetic fuel systems. Together, these subsections support the selection of technologies employed in this study and justify their configuration within the integrated system.

### 2.1. Overview of carbon dioxide emissions from end-use sectors

Building on the urgency for climate-compatible fuels and emerging technological pathways, this section provides background on the distribution of carbon dioxide emissions across major end-use sectors. Understanding sectoral CO<sub>2</sub> sources is essential to identifying where sustainable fuels like e-diesel can have the greatest impact.

As of 2023, industry, transportation, and buildings accounted for roughly 55% of global energy-related CO<sub>2</sub> emissions [20]. While electrification and efficiency are core mitigation strategies, their feasibility varies across sectors. Heavy industry and long-distance transport face persistent barriers to full decarbonization, as many low-carbon alternatives are not yet deployable at scale [21–23]. This highlights the need for complementary solutions, such as synthetic fuels and carbon-capture technologies.

Industrial emissions stem from high-temperature heat and process emissions in cement, steel, and petrochemicals [23]. Transport emissions, driven by aviation, shipping, and freight, have risen steadily since 2010 and dominate energy use in nearly 40% of countries [22]. Decarbonization is hindered by reliance on energy-dense fuels, slow fleet turnover, and limited electrification for long-range modes [24].

Given these challenges, DAC-derived synthetic fuels offer a carbon-neutral option compatible with existing infrastructure, especially vital for sectors unlikely to fully electrify. Their role is increasingly important in pathways toward net-zero emissions.

### 2.2. Brief review of CDR approaches and examination of DAC as a viable CDR pathway

While mitigation remains central to climate action, residual emissions from hard-to-abate sectors — such as heavy industry and long-distance transport — are expected to persist for decades [21,22]. To address these, carbon dioxide removal (CDR) technologies are increasingly viewed as essential complements to emission-reduction strategies. Options range from nature-based solutions to engineered approaches like bioenergy with carbon capture and storage (BECCS), enhanced mineralization, and direct air capture (DAC) [21]. Among them, DAC

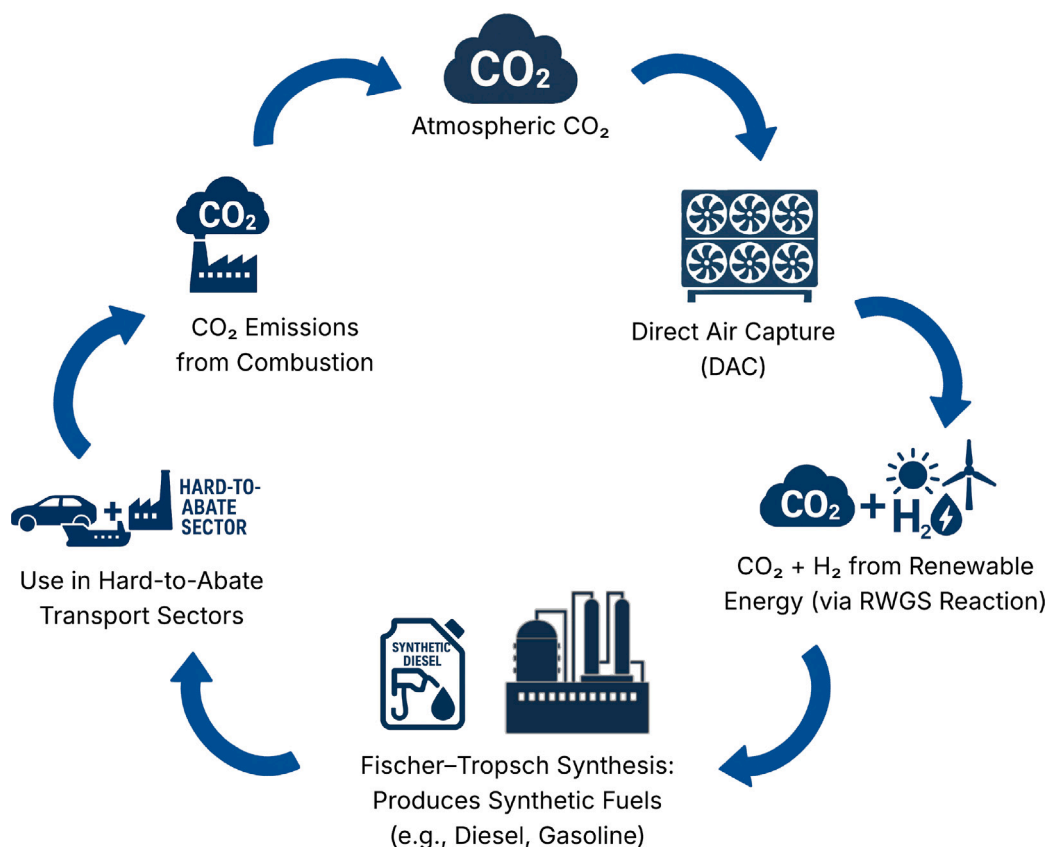


Fig. 1. Schematic of a closed-loop carbon cycle integrating DAC with synthetic fuel production via Fischer–Tropsch synthesis.

stands out for its high scalability and potential to offset emissions where electrification or fuel switching is infeasible [25].

Early work by Keith et al. [26] demonstrated the feasibility of a KOH–Ca loop DAC system. Deutz et al. [27] reported carbon removal efficiencies up to 96% using low-carbon electricity. More recent studies have explored coupling DAC with synthetic fuel production. For instance, Morimoto et al. [28] and Guzman et al. [29] showed that DAC combined with renewable hydrogen and Fischer–Tropsch synthesis (FTS) can achieve greater net CO<sub>2</sub> reductions than flue-gas-based systems. As shown in Fig. 1, this integrated route captures atmospheric CO<sub>2</sub>, converts it to syngas via reverse water-gas shift (RWGS), and upgrades it to liquid fuels like diesel via FTS.

These developments position DAC as a promising source of carbon feedstock for producing low-carbon, drop-in fuels. Still, accurate environmental assessments depend on detailed system modeling and high-resolution carbon flow data.

### 2.3. Review of electrolysis technologies, CO<sub>2</sub> recovery processes, and the Fischer–Tropsch process

To harness the full potential of DAC for synthetic fuel production, it must be integrated with technologies that convert CO<sub>2</sub> and renewable hydrogen into hydrocarbons. The system proposed here relies on three core components: electrolysis for hydrogen generation, CO<sub>2</sub> recovery and purification, and Fischer–Tropsch synthesis (FTS) for fuel production. This section reviews these enabling technologies, emphasizing their principles, benefits, current limitations, and relevance to the DAC-to-e-diesel concept.

#### 2.3.1. Electrolysis technologies

Electrolysis enables sustainable hydrogen production for power-to-gas and synthetic fuel systems. Key approaches include alkaline water electrolysis (AWE), proton exchange membrane (PEM) electrolysis, and

solid oxide electrolysis cells (SOECs), the latter uniquely suited for co-electrolyzing H<sub>2</sub>O and CO<sub>2</sub>.

Alkaline water electrolyzers (AWE) are commercially established due to their low cost, use of non-precious metal catalysts, and suitability for large-scale hydrogen production [30,31]. However, their low current densities, limited dynamic response, and gas crossover issues hinder integration with variable renewable energy sources [32,33]. In contrast, proton exchange membrane (PEM) electrolyzers offer higher current densities and faster response times, making them more compatible with intermittent renewables [34,35]. Despite their performance advantages, PEM systems face challenges such as high capital costs from noble metal catalysts and membrane degradation under dynamic loads [36,37]. Ongoing research targets improved durability and cost reduction in both technologies to support renewable-based hydrogen production at scale [31,33].

Solid oxide electrolysis cells (SOECs) operate at high temperatures and enable direct co-electrolysis of steam and CO<sub>2</sub> to produce syngas [38], making them highly efficient for carbon-neutral fuel synthesis [37,39]. Their elevated operating temperature allows partial substitution of electricity with thermal energy, enhancing overall efficiency [39]. However, SOECs face durability issues due to material degradation from thermal cycling, coking, and redox instability [40,41]. Integration and sealing challenges, along with scale-up limitations, have confined most applications to pilot or demonstration scales [33].

Given their high thermoelectric efficiency and syngas output, SOECs were selected as the core electrolyzer in this study. Their ability to co-electrolyze CO<sub>2</sub> and H<sub>2</sub>O aligns well with FT synthesis requirements, facilitating tighter thermal and material integration. While durability and scale-up remain hurdles, this model aims to explore the theoretical performance and integration potential of SOECs under idealized conditions.

### 2.3.2. CO<sub>2</sub> recovery technologies

CO<sub>2</sub> recovery is essential for carbon capture and utilization (CCU) systems and often precedes FTS to provide high-purity CO<sub>2</sub> or syngas feedstock.

Amine-based absorption, especially with monoethanolamine (MEA), remains the most established CO<sub>2</sub> capture method due to its high selectivity and suitability for post-combustion flue gas treatment [42]. However, high regeneration energy, solvent degradation, corrosion, and volatile emissions pose significant drawbacks [43,44]. Current research aims to enhance solvent stability and reduce energy use through process intensification [42].

Membrane-based CO<sub>2</sub> capture offers compact, modular designs and avoids phase changes, reducing operational complexity [45]. However, limitations include the trade-off between permeability and selectivity, as well as membrane degradation and fouling [46]. Current efforts focus on hybrid systems and advanced materials to improve scalability.

Adsorption methods such as pressure swing adsorption (PSA) and cryogenic separation offer potential energy savings in specific applications [47], but are constrained by sorbent degradation and high energy demand for cryogenics [48]. Ongoing work seeks improved sorbents and optimized cycle designs.

Physical solvents like Selexol and Rectisol rely on physical absorption, making them effective at high CO<sub>2</sub> partial pressures typical of syngas streams [49]. Their lower regeneration energy offers advantages over chemical absorbents, though their performance declines in dilute gas conditions [50]. Research continues on next-generation solvents with broader operating windows.

In this study, a physical solvent-based CO<sub>2</sub> recovery unit was implemented downstream of the SOEC, where syngas contains elevated CO<sub>2</sub> partial pressures. Under these conditions, physical solvents offered an energy-efficient approach to recover unconverted CO<sub>2</sub> for recycle.

### 2.3.3. Fischer–Tropsch fuel synthesis

The Fischer–Tropsch (FT) process catalytically converts syngas into liquid hydrocarbons and plays a central role in synthetic fuel production [51]. Iron- and cobalt-based catalysts are commonly used; iron is often preferred for biomass-derived syngas due to its tolerance to contaminants and promotion of the water–gas shift reaction [52,53]. Despite its maturity, FT synthesis faces issues such as catalyst deactivation from sintering and coking, and sensitivity to H<sub>2</sub>/CO ratios [54,55]. Its economic viability is limited by high capital and operating costs, especially for small-scale plants [56]. Research efforts target catalyst innovation, modular plant designs, and integration with upstream CO<sub>2</sub> capture and co-electrolysis to enhance scalability and lower costs [57].

Electrolysis, CO<sub>2</sub> recovery, and FT synthesis together form the technological core of the proposed DAC-to-e-diesel system. Each contributes critical capabilities while posing trade-offs that shape overall performance and feasibility. From a technology readiness perspective, recent assessments indicate that liquid- and solid-sorbent DAC systems are progressing toward mid-to-high readiness levels (approximately TRL 6–7), with several pilot- and demonstration-scale plants operating continuously, though large-scale commercial deployment remains limited [58]. In contrast, solid oxide electrolysis — particularly CO<sub>2</sub>/H<sub>2</sub>O co-electrolysis — remains at a lower TRL, with material degradation, thermal cycling, and long-term stack durability identified as key challenges to industrial deployment [59].

Recognizing these differing maturity levels is essential for identifying realistic integration opportunities and for interpreting the results of system-level modeling. The preceding review therefore provides the basis for the technology selection and integration strategy adopted in this study, which aims to explore performance synergies and energy-efficiency potential under idealized but literature-consistent operating assumptions.

### 2.4. Life cycle CO<sub>2</sub> emissions background for synthetic fuel systems

Accurately estimating life cycle CO<sub>2</sub> emissions is essential for evaluating the climate benefits of synthetic fuel pathways, particularly those involving direct air capture (DAC) and Fischer–Tropsch synthesis. Several prior studies have analyzed synthetic fuels produced from captured CO<sub>2</sub> and renewable hydrogen, including DAC-based diesel. For instance, Liu et al. [60] have reported cradle-to-grave CO<sub>2</sub> emissions as low as 12 g-CO<sub>2</sub>eq./MJ under clean electricity assumptions, but their work is based on pilot-scale data with little information about fuel synthesis. Similarly, Deutz and Bardow [27] have characterized operational DAC performance without extending the analysis to fuel conversion or end-use.

Broader carbon balance studies on synthetic fuels from captured CO<sub>2</sub> have been conducted [61–63], though many suffer from ambiguous system boundaries and assumptions. Reviews by Hepburn et al. [64] and Minx et al. [65] highlight ongoing issues with transparency and consistency. Process simulation-based assessments [66,67] offer improved accuracy, but standardization of functional units and co-product allocation remains a challenge.

Recent work by Morimoto et al. [28] combines techno-economic analysis with life cycle assessment for synthetic fuels, but often lacks diesel-specific modeling detail. LCAs of bio- and waste-based diesel alternatives, such as those from biomass or landfill gas [68,69], reveal trade-offs related to feedstock availability and indirect emissions, underscoring the need to assess non-biogenic synthetic fuels.

This study adopts a life-cycle CO<sub>2</sub> framework tailored to the DAC–SOEC–FT diesel pathway, quantifying emissions across capture, electrolysis, synthesis, upgrading, and end use, with the aim of enabling transparent evaluation for hard-to-abate sectors.

## 3. Methodology

To evaluate the environmental feasibility of producing synthetic diesel (e-diesel) from atmospheric CO<sub>2</sub>, cradle-to-gate CO<sub>2</sub> emissions were estimated. This system boundary includes all foreground operations and upstream energy inputs required to produce one tonne of e-diesel at the refinery gate. Following DAC-specific LCA guidance from the U.S. Department of Energy [70], the analysis encompasses ambient air capture using a liquid-sorbent-based DAC system, oxygen supply via a cryogenic ASU, hydrogen generation through SOEC co-electrolysis, syngas conditioning, Fischer–Tropsch synthesis, product separation and upgrading, as well as internal CO<sub>2</sub> recovery and recycling. Background emission factors for electricity and fuel use were obtained from established inventory databases. Consistent with recommendations for early-stage technologies, the analysis adopts an attributional approach and excludes infrastructure, land use, and distribution stages. The functional unit, one tonne of synthetic diesel, is aligned with standards from the Global CO<sub>2</sub> Initiative [71] and the IEA GHG Program [72], enabling consistent comparison of carbon intensity across integrated synthetic fuel pathways.

The analysis focused on three key aspects: (i) quantifying energy demand across major subsystems, (ii) estimating direct and indirect CO<sub>2</sub> emissions from both foreground processes and background energy sources, and (iii) assessing the integration potential of critical technologies involved in DAC-derived e-diesel production. The accounting of emissions emphasized energy-related contributions within the modeled major system, while carbon intensity factors associated with ancillary electricity and fuel inputs were sourced from the literature.

To support this analysis, we consistently applied a cradle-to-gate system boundary across all scenarios to capture upstream energy inputs and requirements for DAC, hydrogen production, syngas processing, and fuel synthesis. The modeling framework followed an equation-oriented approach to evaluate energy and carbon flows under steady-state conditions.

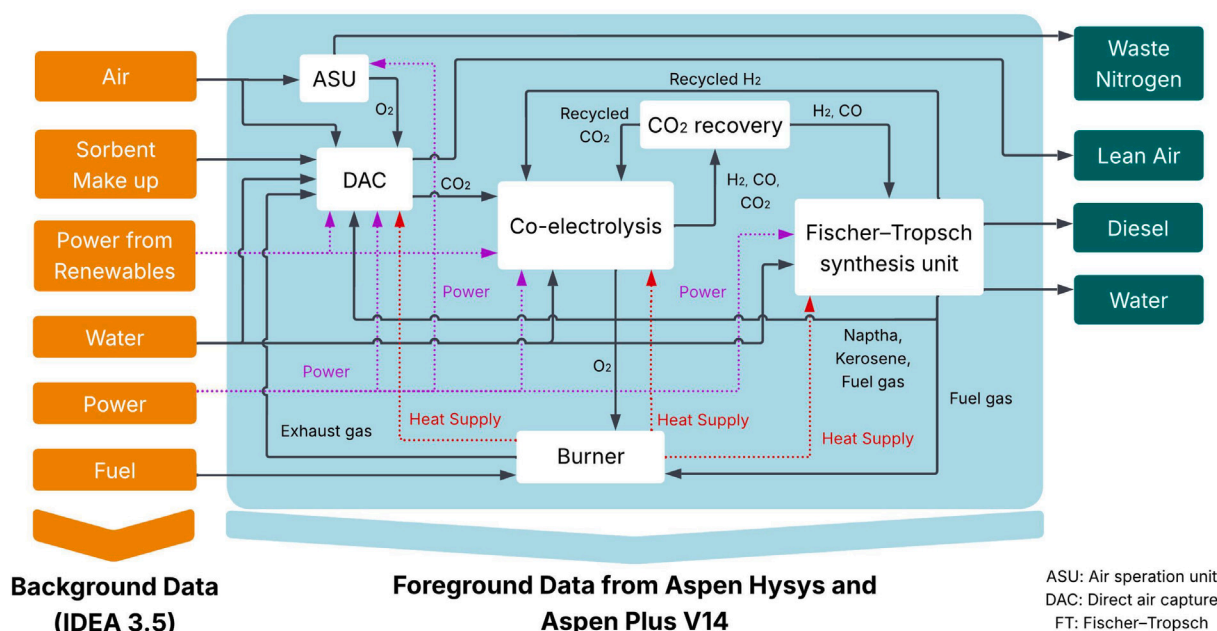


Fig. 2. Process flow and system boundary for the production of diesel using direct air capture (DAC).

### 3.1. Integrated process design and simulation setup

After describing the framework for estimating emissions, this section details the configuration and simulation of the integrated DAC-to-diesel production system to be modeled. The process design draws from the established literature on synthetic fuel production from captured CO<sub>2</sub> and renewable hydrogen [73–77], and it reflects the operational assumptions and boundaries previously depicted in Fig. 2. In the base case, the SOEC electrolyzer is assumed to operate on dedicated renewable electricity (e.g., solar or wind), reflecting its role as the primary hydrogen source. All other process units are assumed to use conventionally generated electricity and thermal energy. While the intermittency of renewables and equipment degradation are not explicitly modeled, this partial off-grid configuration allows for evaluating the system's internal integration potential under steady-state conditions. Additional simplifying assumptions include idealized heat transfer (no external losses), negligible pressure drops across units, and uniform reactor performance without spatial gradients. These approximations are typical in conceptual-level modeling and enable a first-order assessment of energy balances and integration opportunities.

As depicted in Fig. 3, the proposed system integrates four major subsystems into a unified process flow: (a) a liquid-sorbent-based DAC unit with a cryogenic air separation unit (ASU) for oxygen supply, following the configuration proposed by Keith et al. [26]; (b) a solid oxide electrolysis cell (SOEC) system for co-electrolyzing CO<sub>2</sub> and steam to produce syngas; (c) a physical solvent-based module for CO<sub>2</sub> recovery and compression; and (d) a Fischer-Tropsch (FT) synthesis unit for converting syngas into diesel-range hydrocarbons. These subsystems were modeled using a commercial, equation-oriented steady-state simulation platform to estimate mass and energy balances, assess unit-level synergies, and quantify carbon flows across the integrated system. To complement the overall process flow diagram shown in Fig. 3, detailed schematic representations of each subsystem, including material and heat streams, are provided in Figs. 4, 5, and 6.

To assess the potential for internal energy reuse, a conceptual heat integration analysis was conducted based on simulation outputs. All major process streams were evaluated to identify available heat sources and their corresponding temperature ranges, as well as the temperature and duty requirements of key heat sinks. Hot and cold streams were then systematically matched according to established heat

integration heuristics, ensuring that heat was transferred from higher- to lower-temperature streams without any temperature cross within the exchanger. Exothermic reactor heat was only integrated when the source temperature exceeded that of the target stream, thereby respecting thermodynamic feasibility and preserving directionality of heat flow. This analysis was intended as a screening-level assessment to identify physically plausible integration opportunities across subsystems. The detailed temperature and duty ranges of all matched streams are summarized in Table S3.

For the process design, the DAC is used to capture CO<sub>2</sub> from ambient air, and a cryogenic ASU is used to supply oxygen for combustion in the calciner unit to generate heat [26]. In co-electrolysis using SOEC, both steam (H<sub>2</sub>O) and carbon dioxide (CO<sub>2</sub>) are simultaneously electrolyzed at high temperatures to generate H<sub>2</sub> and CO (cathode) and O<sub>2</sub> (anode) [78]. The resulting syngas (a mixture of CO and H<sub>2</sub>), along with residual CO<sub>2</sub>, is compressed and sent to the CO<sub>2</sub> recovery unit for CO<sub>2</sub> separation [79].

The syngas stream exiting the CO<sub>2</sub> recovery unit is routed to the FT synthesis process, where it is converted into a range of hydrocarbons, including naphtha (C<sub>5</sub>–C<sub>6</sub>), gasoline (C<sub>7</sub>–C<sub>10</sub>), and diesel-range products (C<sub>11</sub>–C<sub>19</sub>) [80–82]. The hydrogen produced via pressure swing adsorption (PSA) from the FT tail gas is recycled internally to support hydrocracking within the FTS unit and to supplement the co-electrolysis process in the SOEC system.

A key innovation of the proposed configuration was the strategic utilization of hydrocarbon byproducts, specifically, naphtha, kerosene, and fuel gas, as a combustion fuel, for the oxy-fired calciner in the DAC system. This thermochemical coupling not only offsets the need for external fuel sources but also enhances process integration by valorizing internal streams that would otherwise have required further separation or disposal. As a result, the improved thermal efficiency and carbon circularity achieved by the system supported the goal of minimizing net emissions across the integrated DAC–e–diesel pathway.

The remaining gasoline and off-gases from the PSA unit were used as burner fuel to supply thermal energy for the SOEC and FTS subsystems. To further reduce reliance on external heat sources, heat integration was applied throughout the system wherever feasible to enable recovery and redistribution of thermal energy between high-temperature units [83–85]. This design approach contributed to enhanced overall energy efficiency and supported the system's goal of maximizing internal resource utilization.

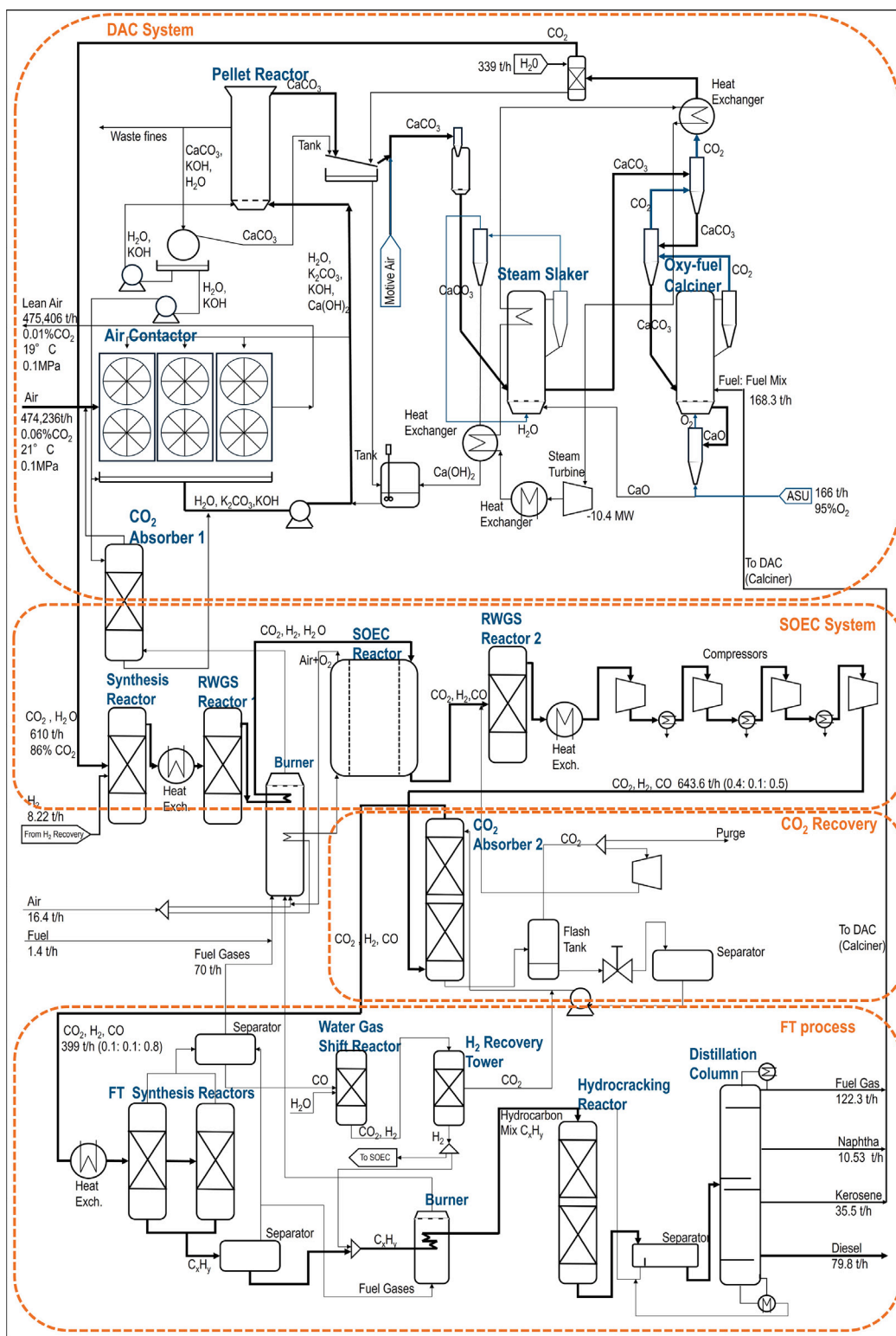


Fig. 3. Integrated process flow diagram for synthetic diesel production via DAC, SOEC, and FT synthesis.

Fig. 4 presents the detailed configuration of the DAC system used for capturing CO<sub>2</sub> from ambient air, along with the integrated ASU that supplies oxygen for the calciner. The DAC layout followed the design proposed by Keith et al. (2018) [26] and comprised four major components: the air contactor, pellet reactor, slaker, and calciner [86].

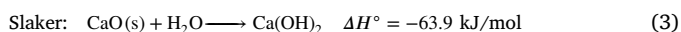
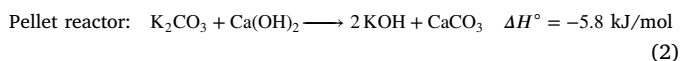
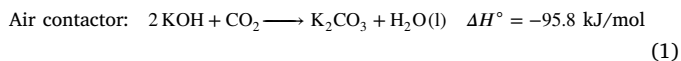
The process design begins with the intake of atmospheric air, containing approximately 0.06 wt% CO<sub>2</sub>, into the air contactor [26]. To enhance overall capture efficiency, this stream is supplemented with flue gases from the SOEC and FT synthesis units, which contain elevated CO<sub>2</sub> concentrations of 16.1 and 29.6 wt%, respectively. Within

the air contactor, CO<sub>2</sub> from both sources reacts with potassium hydroxide (KOH) to form potassium carbonate (K<sub>2</sub>CO<sub>3</sub>), as described in Reaction (1) [87].

The resulting K<sub>2</sub>CO<sub>3</sub> solution is directed to the pellet reactor, where it reacts with calcium hydroxide (Ca(OH)<sub>2</sub>), along with recirculated CaCO<sub>3</sub> seed crystals from the calciner, to regenerate KOH and precipitate calcium carbonate (CaCO<sub>3</sub>) (Reaction (2)). The solid CaCO<sub>3</sub> is separated and sent to the calciner, while the regenerated KOH is recycled back to the air contactor.

In the calciner, CaCO<sub>3</sub> undergoes thermal decomposition to produce calcium oxide (CaO) and concentrated CO<sub>2</sub> (Reaction (4)) [88]. The required heat is supplied by complete combustion of FT byproducts — naphtha and tail gases — using high-purity oxygen from the ASU. This oxy-fuel combustion approach, originally adopted in the design by Keith et al. [89], ensures that the combustion products are primarily CO<sub>2</sub> and H<sub>2</sub>O, thereby avoiding the dilution effect of nitrogen present in air. This eliminates the need for downstream separation of CO<sub>2</sub> from flue gas and allows direct recycling of concentrated CO<sub>2</sub> into the DAC system. Using air or oxygen-enriched air instead would introduce nitrogen, leading to a mixed flue gas and complicating both CO<sub>2</sub> purification and system integration. The calciner output includes CaO, CO<sub>2</sub>, and residual CaCO<sub>3</sub>. The solid CaO is then sent to the slaker, where it reacts with water vapor — preheated using heat recovery from the slaker outlet — to form fresh Ca(OH)<sub>2</sub> for reuse in the pellet reactor (Reaction (3)) [90].

Finally, the captured CO<sub>2</sub> is washed in a knockout drum and directed to the SOEC unit for conversion into syngas. The integration of flue gases and internal fuel combustion enables deep CO<sub>2</sub> removal, lowering the concentration in the air contactor exhaust to 0.012 wt%. The full set of reactions involved in the DAC process is summarized below [90].



Pressurized water at 42 bar is first preheated using thermal energy recovered from the slaker outlet and then superheated to 415 °C using exhaust heat from the calciner. The electricity produced from this steam is used to power components within the DAC loop, including the main air compressor used for fluidization, thereby reducing the demand for external electricity.

Fig. 5 illustrates the integrated co-electrolysis (SOEC) process, which combines synthesis reactions, a two-stage reverse water–gas shift (RWGS) sequence, and high-temperature electrochemical conversion. The input gas stream consists of H<sub>2</sub>O, CO<sub>2</sub>, O<sub>2</sub>, and N<sub>2</sub> from the DAC unit, along with high-purity H<sub>2</sub> recovered from the FT synthesis purge stream (85% recovery, 99.99% purity via PSA). The gas composition is configured to maintain a steam-to-carbon (S/C) ratio above 1.5 at the SOEC inlet, a condition known to suppress carbon formation and ensure stable operation of Ni-based cathodes under co-electrolysis conditions [91–93]. This gas mixture is compressed to 2 bar before entering the pre-treatment section.

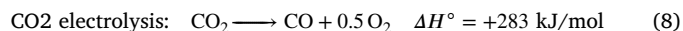
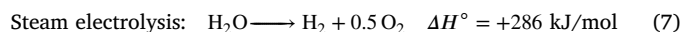
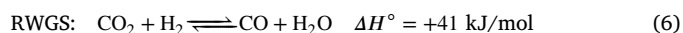
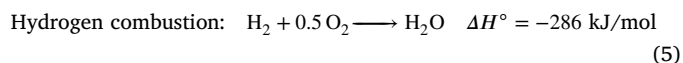
In the synthesis step, H<sub>2</sub> reacts with residual O<sub>2</sub> to form H<sub>2</sub>O (Reaction (5)), which is then combined with additional CO<sub>2</sub> and heated to 800 °C using heat from a dedicated burner. The hot gas enters the first low-temperature RWGS reactor, where some of the CO<sub>2</sub> is catalytically converted to CO (Reaction (6)) [94].

This configuration employs a two-stage RWGS arrangement in combination with co-electrolysis to enhance conversion efficiency and support stable SOEC operation. The first RWGS reactor acts as a thermal pre-conditioning step, partially converting CO<sub>2</sub> before it enters the electrolyzer. This helps moderate the inlet composition and temperature,

reducing the risk of carbon deposition in the SOEC. A second RWGS reactor downstream of the SOEC further upgrades the gas mixture, converting residual CO<sub>2</sub> using excess H<sub>2</sub>, thereby increasing overall syngas yield.

The partially converted gas stream, containing CO<sub>2</sub> and H<sub>2</sub>O, is then introduced into the SOEC unit, which enables simultaneous high-temperature electrochemical reduction of both species to syngas (H<sub>2</sub> and CO). This step provides thermodynamic synergy and avoids the need for separate hydrogen and CO production pathways. (Reactions (6) and (7)) [93]. The SOEC stack employs a nickel/yttria-stabilized zirconia (Ni/YSZ) cathode, a YSZ electrolyte, and a lanthanum strontium cobalt oxide/ceria-gadolinia oxide (LSC/CGO) anode [95], selected for high ionic conductivity and thermal stability under reducing conditions.

The oxygen produced is routed to the system burner to combust FT tail gas, a minor gasoline fraction, and additional air, supplying the thermal energy required by the RWGS and SOEC units. The syngas-rich stream exiting the SOEC is routed to a second RWGS reactor to further convert residual CO<sub>2</sub> in the presence of excess H<sub>2</sub> [93]. Finally, the resulting gas mixture, comprising H<sub>2</sub>, CO, and unconverted CO<sub>2</sub>, is compressed to 30 bar and sent to the CO<sub>2</sub> recovery unit, where CO<sub>2</sub> is separated and recycled back into the system. The complete set of reactions for the integrated co-electrolysis process is summarized below [28,96]:



Unreacted CO<sub>2</sub> in the co-electrolysis outlet stream is separated and recycled using a physical absorption process based on Selexol<sup>®</sup>, a dimethyl ether of polyethylene glycol solvent [97]. The gas mixture containing CO<sub>2</sub>, CO, and H<sub>2</sub> enters an absorber column, where cold lean solvent selectively absorbs CO<sub>2</sub> [98]. The subsequent expansion of the CO<sub>2</sub>-rich solvent is then expanded to 13.8 bar, allowing unabsorbed CO and H<sub>2</sub> to be recovered in a flash tank, compressed, and recycled. CO<sub>2</sub> is released from the solvent through a staged flash process down to 1.01 bar, after which the regenerated solvent is pressurized, cooled, and returned to the absorber. The recovered CO<sub>2</sub> is compressed to 3.5 bar and recycled to the SOEC unit [98]. The cleaned syngas, now at 30 bar, is directed to the FT synthesis reactor.

As shown in Fig. 5, heat integration is implemented within the SOEC and CO<sub>2</sub> recovery system to improve energy efficiency. The outlet stream from the second RWGS reactor is used to preheat the inlet of the first RWGS reactor to 483 °C. High-temperature heat from the burner (1756 °C) is used to raise the gas feed to 800 °C and to preheat burner air.

Fig. 6 depicts the FT synthesis unit, where syngas (CO and H<sub>2</sub>) is catalytically converted into a broad range of hydrocarbons, from methane to long-chain waxes [80,86]. The reaction proceeds via –CH<sub>2</sub>– unit polymerization (Eq. (9)), with product distribution modeled by the Anderson–Schulz–Flory (ASF) equation (Eq. (13)) using a chain growth probability ( $\alpha$ ) of 0.91 [28]. This relatively high  $\alpha$  value was selected to favor the formation of long-chain hydrocarbons, primarily waxes, which are subsequently converted into diesel-range fuels through hydrocracking. Although lower  $\alpha$  values would shift product distribution toward lighter hydrocarbons, targeting waxes at the FT stage allows greater flexibility and control over the final product spectrum, as heavier fractions can be upgraded with high selectivity to diesel. Simplified overall reactions are given in Eqs. (10) and (11).

Diesel production is maximized through the selection of appropriate catalysts and operating conditions, with cobalt-based catalysts favored

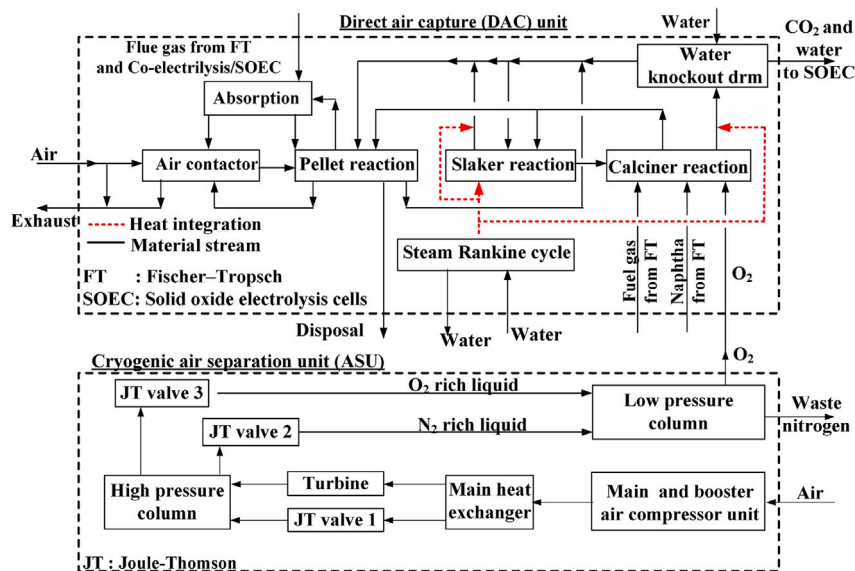
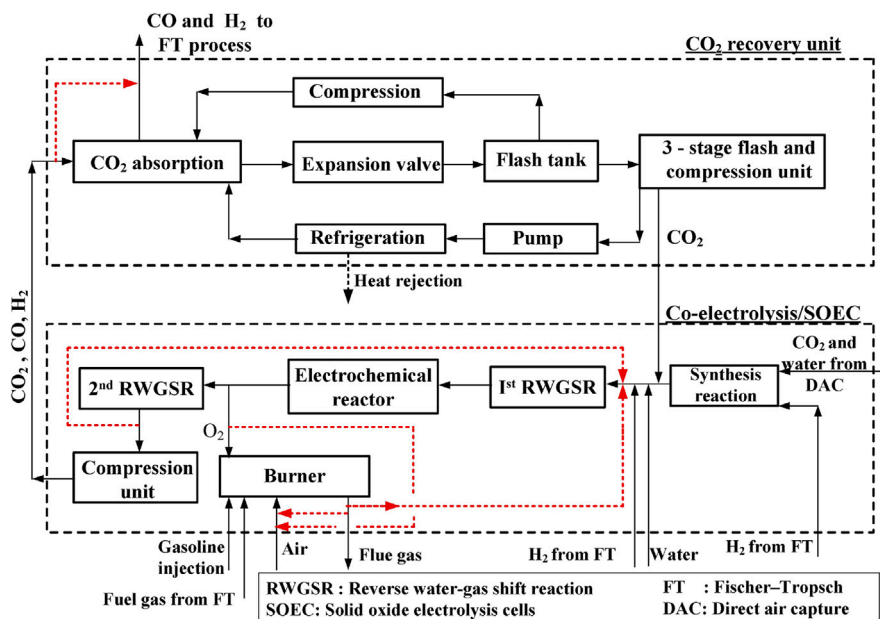


Fig. 4. Detailed subsystem diagram of DAC and ASU with heat integration.

Fig. 5. Detailed subsystem diagram of SOEC and CO<sub>2</sub> recovery with heat integration.

for mid-carbon-range products [80,99,100]. In this study, the FT reactor was modeled as a fixed-bed reactor system operating at 230 °C and 30 bar, consistent with common industrial designs employing cobalt-based catalysts for high  $\alpha$  values and diesel-range selectivity [80,99]. The reported 87% CO conversion corresponds to the overall conversion efficiency, including internal gas recycle to increase syngas utilization. Recycle of unconverted light gases enables deeper conversion and improves the yield of heavier hydrocarbons while minimizing CO vent losses.

The FT reactor effluent is cooled to condense heavy hydrocarbons and water, while unconverted gases are sent to a water-gas shift (WGS) reactor to enhance H<sub>2</sub> yield [101]. Recovered hydrogen is separated via pressure swing adsorption and recycled to both the FT reactor and SOEC unit.

Heavier hydrocarbons, primarily long-chain waxes, are directed to a hydrocracking unit where they undergo catalytic hydrogenation to produce lighter, more valuable fractions. The resulting product mixture is

subsequently separated via fractional distillation into four main hydrocarbon cuts: fuel gases (C<sub>1</sub>–C<sub>4</sub>), naphtha (C<sub>5</sub>–C<sub>6</sub>), kerosene/gasoline cut (C<sub>7</sub>–C<sub>10</sub>), and diesel (C<sub>11</sub>–C<sub>19</sub>). Unconverted waxes or heavy residues are recycled back to the hydrocracker to improve overall conversion efficiency and product yield uniformity.

A portion of the naphtha, purge gas, and gasoline fractions is combusted to provide thermal energy for the DAC calciner, while the remaining PSA off-gases and gasoline are used to supply heat to the SOEC and FT units. The key chemical reactions involved in the FT and WGS processes are listed below [28,101–103].

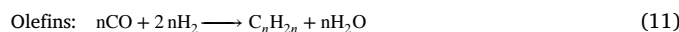
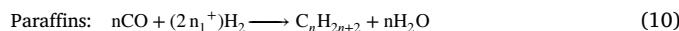
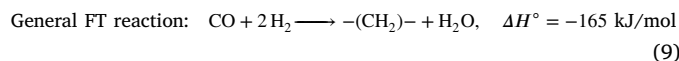




**Table 1**  
Property method and the temperature and pressure of the reactors used in the simulation (in Aspen Plus® V14) for the production of diesel using direct air capture (DAC).

Parameters	Process Unit	Component	Value	
Property method	DAC [26,105–107]	Air contactor and pellet reactor	ELECNRTL	
		Calciner	RK-SOAVE	
		Slaker	RK-SOAVE	
		Cryogenic ASU [75]	All components	Peng–Robinson
		Co-electrolysis/SOEC [84,108,109]	All components	Peng–Robinson
Temperature and pressure	CO <sub>2</sub> recovery [79]	All components	PC-SAFT	
		FT process [76,110,111]	All components	Peng–Robinson
		DAC [88,90,112–114]	Air contactor and pellet reactor	21.0 °C & 1.0 bar
	Co-electrolysis/SOEC [80,93,96,104,108,111]	Calciner	900 °C & 1.6 bar	
		Slaker	300 °C & 1.6 bar	
		Synthesis reaction	109 °C & 2.0 bar	
		1st RWGS reactor	300 °C & 1.6 bar	
		2nd RWGS reactor	800 °C & 1.6 bar	
		Electrochemical reduction	800 °C & 1.6 bar	
		FT process [76,80,86,101,102]	FT synthesis reactor	230 °C & 25 bar
WGS reactor	250 °C & 25 bar			
Hydrocracker	315 °C & 50 bar			

**Table 2**  
Assumptions used for the simulation of DAC, ASU, SOEC, CO<sub>2</sub> recovery and FT process in Aspen Plus® V14 and Aspen HYSYS® V14.

Process Unit	Parameter	Value
DAC [26,84,88]	Flow rate of air	472,248 t/h
	Percentage of CO <sub>2</sub> in air	0.06 wt%
	Inlet temperature and pressure of air	25.0 °C & 1.01 bar
	Conversion coefficient CaCO <sub>3</sub> in calciner	0.98
	Conversion coefficient to CaO in slaker	0.85
ASU [26,115,116]	Mass flowrate of air	767 t/h
	Inlet temperature and pressure of air	25.0 °C & 1.01 bar
	Exit temperature of air from intercooler and after-cooler	30.0 °C
	Hot end approach and pinch temperature	3.0 °C & 2.8 °C
	Flow rate and purity of oxygen	166 t/h and 95.6%
SOEC [84,93,117]	O <sub>2</sub> conversion coefficient in synthesis	1.00
	CO <sub>2</sub> conv. in electrochemical reduction	0.05
	H <sub>2</sub> O conv. in electrochemical reduction	0.98
	Inlet temperature and pressure of air and water	25.0 °C & 1.01 bar
CO <sub>2</sub> recovery [79,97,98]	Absorber pressure and temperature	30 bar & 27 °C
	HP, MP and LP flash drum pressure	3.50, 1.00, and 0.27 bar
	Lean solvent cooling temperature	−1.11 °C
FT process [84,118]	Overall Conversion of CO in FT system	0.87
	Inlet temperature and pressure of air and water	25.0 °C & 1.01 bar

**Required total heat with heat integration.** When thermal integration between process units is implemented, the overall heat demand is reduced as described below:

$$\dot{Q}_{\text{Total (WHI)}} = \dot{Q}_{\text{DAC,req(WHI)}} + \dot{Q}_{\text{SOEC,req(WHI)}} + \dot{Q}_{\text{CO2,recov,req(WHI)}} + \dot{Q}_{\text{FT,req(WHI)}} \quad (29)$$

**Required total power consumption.** The total power requirement of the integrated system accounts for the electricity consumed by all subsystems and the power generated within the DAC module:

$$\dot{W}_{\text{Total}} = \dot{W}_{\text{DAC,req}} + \dot{W}_{\text{ASU,req}} + \dot{W}_{\text{SOEC,req}} + \dot{W}_{\text{CO2,recov,req}} + \dot{W}_{\text{FT,req}} - \dot{W}_{\text{DAC,gen}} \quad (30)$$

### 3.4. Cradle-to-gate estimation of CO<sub>2</sub> emission

In alignment with the methodological framework introduced in Section 2.4, we applied a streamlined life cycle CO<sub>2</sub> emission estimation method tailored to the DAC–hydrogen–FT diesel pathway. We

focused on evaluating carbon intensity across the key process stages, direct air capture, water electrolysis, and FTS, clearly defined operating conditions (see Fig. 2).

For each scenario, we quantified demands for energy (electricity and heat) and materials, and we estimated their associated carbon footprints in terms of total CO<sub>2</sub> emissions per tonne of diesel produced. Emission calculations combined both upstream emissions from material and energy inputs and direct process emissions, as expressed by:

$$EM_{\text{total}} = \sum_i (m_i \cdot I_i) + EM_h \quad (31)$$

Here,  $m_i$  denotes the mass of input  $i$ ,  $I_i$  its emission intensity, and  $EM_h$  the direct emissions arising within the production system. Table 5 summarizes the process input quantities per tonne of diesel product, derived from process simulations using Aspen Plus V14®. Emission intensity data for grid electricity in Japan and Canada were obtained from the International Energy Agency (IEA) [119], while data for other inputs, such as raw materials and water, were sourced from the IDEA 3.5 Database [120]. These background data were used to calculate the cradle-to-gate CO<sub>2</sub> emissions associated with each scenario. This

**Table 3**  
Heat requirement in DAC, SOEC, CO<sub>2</sub> recovery and FT process without and with heat integration (WOHI & WHI).

Heat requirement in DAC (in MW)	
$\dot{Q}_{DAC\_req(WOHI)} = \dot{Q}_{RC\_E}$	(15)
where $\dot{Q}_{RC\_E}$ is the required heat for evaporation and the superheat of water in RC.	
$\dot{Q}_{DAC\_req(WHI)} = \dot{Q}_{DAC\_req(WOHI)} - \dot{Q}_{Reactor\_out} - \dot{Q}_{Reactor}$	(16)
where $\dot{Q}_{Reactor\_out}$ is recovered heat from the calciner and slaker outlet stream; $\dot{Q}_{Reactor}$ is removed heat from slaker unit.	
Heat requirement in SOEC (in MW)	
$\dot{Q}_{SOEC\_req(WOHI)} = \dot{Q}_{Reactor\_inlet} + \dot{Q}_{Burner\_air\_inlet} + \dot{Q}_{Reactor}$	(17)
where $\dot{Q}_{Reactor\_inlet}$ is the required heat to the inlet of the first RWGS reactor and electrochemical unit; $\dot{Q}_{Burner\_air\_inlet}$ is the required heat to preheat air; $\dot{Q}_{Reactor}$ is the required heat in the second RWGS reactor and electrochemical reactions.	
$\dot{Q}_{SOEC\_req(WHI)} = \dot{Q}_{SOEC\_req(WOHI)} - \dot{Q}_{Burner\_out} - \dot{Q}_{Reactor\_out} - \dot{Q}_{Reactor}$	(18)
where $\dot{Q}_{Burner\_out}$ is recovered heat from the burner outlet; $\dot{Q}_{Reactor\_out}$ from second RWGS and electrochemical unit; $\dot{Q}_{Reactor}$ from first RWGS.	
Heat requirement in CO <sub>2</sub> recovery (in MW)	
$\dot{Q}_{CO2\_recov\_req(WOHI)} = \dot{Q}_{CO2\_recov\_syngas}$	(19)
where $\dot{Q}_{CO2\_recov\_syngas}$ is the heat required to preheat syngas before entering FT.	
$\dot{Q}_{CO2\_recov\_req(WHI)} = \dot{Q}_{CO2\_recov\_req(WOHI)} - \dot{Q}_{CO2\_recov\_inlet}$	(20)
where $\dot{Q}_{CO2\_recov\_inlet}$ is recovered heat from absorber inlet used to preheat syngas.	
Heat requirement in FT process (in MW)	
$\dot{Q}_{FT\_req(WOHI)} = \dot{Q}_{Reactor\_inlet} + \dot{Q}_{Separator} + \dot{Q}_{PSA} + \dot{Q}_{Reboiler}$	(21)
where $\dot{Q}_{Reactor\_inlet}$ for FT and hydrocracker; $\dot{Q}_{Separator}$ covers separation; $\dot{Q}_{PSA}$ and $\dot{Q}_{Reboiler}$ are for PSA and reboiler.	
$\dot{Q}_{FT\_req(WHI)} = \dot{Q}_{FT\_req(WOHI)} - \dot{Q}_{Reactor\_outlet} - \dot{Q}_{Burner\_outlet} - \dot{Q}_{Reactor} - \dot{Q}_{Diesel\_outlet}$	(22)
where $\dot{Q}_{Reactor\_outlet}$ and $\dot{Q}_{Burner\_outlet}$ are recovered from FT/WGS outlets and burner; $\dot{Q}_{Reactor}$ is reused heat; $\dot{Q}_{Diesel\_outlet}$ from diesel product stream.	

scenario-based approach enables a transparent comparison of decarbonization potential across different diesel production configurations within hard-to-abate transport applications.

#### 4. Results and discussion

The simulation results for the DAC–SOEC–FT diesel production pathway are summarized in Table 6, which presents electricity and heat demands across each major process unit, with and without heat integration. All values are reported on a per-ton-of-diesel basis.

The DAC subsystem, including CO<sub>2</sub> capture, purification, and compression, accounts for a substantial portion of energy use, 1.13 MWh/t of electricity and 2.27 MWh/t of thermal energy, primarily due to the air separation unit and high-pressure CO<sub>2</sub> compression. The FT process and product upgrading stages also contribute significantly, with 0.19 MWh/t of electricity and up to 2.03 MWh/t of thermal energy required, driven by hydrogen compression, syngas conditioning, and hydrocracking. Electrical energy demand is dominated by the SOEC unit, which requires 29.82 MWh/t, accounting for more than 95% of the system's total electricity load. Although internal electricity recovery remains modest overall (5%), it offsets up to 26% of the DAC's power requirements and provides meaningful auxiliary support. On the thermal side, the non-integrated configuration exhibits a net heat demand of 11.20 MWh/t, which decreases to 3.66 MWh/t under heat integration. This reduction is enabled by recovery from the calciner, SOEC burner, and the exothermic FT reactor. Integration allows 87%

of the SOEC's and 93%–100% of the FT unit's heat demand to be met internally. The DAC system recovers 50% of its heat requirement via combustion of by-products in the oxy-fired calciner, which also drives a Rankine cycle for electricity generation. Overall, the integrated configuration achieves a 78% system-wide heat recovery rate and demonstrates strong thermodynamic synergy between subsystems. This level of integration significantly reduces reliance on external utilities and enhances the energy and carbon efficiency of DAC-derived synthetic diesel production.

To complement the quantitative results, Fig. 7 presents Sankey diagrams comparing the distribution of electricity and thermal energy in the DAC–SOEC–FT system for two configurations: without heat integration (Panel A) and with heat integration (Panel B). By providing a visualization of energy contributions from external utilities and internal recovery, the diagrams highlight process-level allocations across DAC, co-electrolysis, CO<sub>2</sub> recovery, and FT synthesis.

Importantly, the energy flows associated with the SOEC unit reflect only the portion supplied by internal sources, namely, recovered heat and electricity from DAC and FT subsystems. The total energy demand of the SOEC system (29.82 MWh/t-diesel) is substantially larger and is not fully represented in the diagram due to scale adjustments. Nevertheless, the visualization clearly illustrates that integrated heat recovery substantially increases the contribution of internally available energy to the SOEC, thereby reducing its net dependency on external renewable electricity. For example, in the integrated case, 8.63 MWh/t-diesel of heat and 1.08 MWh/t-diesel of electricity are recovered and

**Table 4**  
Required power in DAC, ASU, SOEC, CO<sub>2</sub> recovery and FT process.

Power requirement in DAC (in MW)	
$\dot{W}_{DAC,req} = \dot{W}_{F,p} + \dot{W}_{Cont,p} + \dot{W}_{RC,p} + \dot{W}_{Steam,C}$	(23)
Where, $\dot{W}_{F,p}$ is required power for fan; $\dot{W}_{Cont,p}$ and $\dot{W}_{RC,p}$ are power requirements for pump in contactor and RC, respectively; $\dot{W}_{Steam,C}$ is required power in steam compressor before entering the slaker.	
Power requirement in ASU (in MW)	
$\dot{W}_{ASU,req} = \dot{W}_{MAC} + \dot{W}_{BAC} - \dot{W}_{Air,t}$	(24)
Where, $\dot{W}_{MAC}$ is required power in main air compressor unit; $\dot{W}_{BAC}$ is required power in booster air compressor unit; $\dot{W}_{Air,t}$ is generated power by the air turbine.	
Power requirement in Co-electrolysis/SOEC (in MW)	
$\dot{W}_{SOEC,req} = \dot{W}_{CO_2,C} + \dot{W}_{Air,C} + \dot{W}_{Syngas,C} + \dot{W}_{Water,p}$	(25)
Where, $\dot{W}_{CO_2,C}$ , $\dot{W}_{Air,C}$ and $\dot{W}_{Syngas,C}$ are the compressor power in CO <sub>2</sub> , air, and syngas respectively; $\dot{W}_{Water,p}$ is the power required by the water pump.	
Power requirement in CO <sub>2</sub> recovery unit (in MW)	
$\dot{W}_{CO_2,recov,req} = \dot{W}_{CO_2,C} + \dot{W}_{Recycle,C} + \dot{W}_{DEPG,p}$	(26)
Where, $\dot{W}_{CO_2,C}$ is the power required for CO <sub>2</sub> compression; $\dot{W}_{Recycle,C}$ is the power required in recycle stream to the absorber; $\dot{W}_{DEPG,p}$ is the power required for the DEPG pump.	
Power requirement in FT process (in MW)	
$\dot{W}_{FT,req} = \dot{W}_{H_2,C} + \dot{W}_{Wax,p}$	(27)
Where, $\dot{W}_{H_2,C}$ is the power required for H <sub>2</sub> compression; $\dot{W}_{Wax,p}$ is the pump power required to pressurize wax.	

**Table 5**  
Process inputs for the DAC and SOEC–FT system per tonne of diesel product.

Process Unit	Parameter	Value	Unit
DAC	CO <sub>2</sub> captured	6.6	t/t-product
	Water	19.3	t/t-product
	CaCO <sub>3</sub>	0.117	t/t-product
	KOH	0.0002	t/t-product
	Reused fuel (FT-derived)	180.8	MW
SOEC and FT process	Electricity	1.6	MWh/t-product
	Water	1.3	t/t-product
	Oxygen	2.1	t/t-product
	Reused fuel (FT-derived)	244.7	MW

**Note:** “Reused fuel (FT-derived)” refers to internally recovered naphtha, gasoline, and purge gas streams reused for combustion or heating within the DAC and SOEC–FT system. These are omitted from the material balance as they circulate within a closed-loop process.

directed toward SOEC operation, compared to just 3.07 MWh/t-diesel of heat and 1.08 MWh/t-diesel combined in the non-integrated case.

The effect of integration is also evident in the FT and DAC subsystems. In Panel A (non-integrated), combustion-derived heat from FT by-products is heavily relied upon, particularly for SOEC (6.82 MWh/t-diesel) and FT process (1.89 MWh/t-diesel). In contrast, Panel B (integrated) demonstrates substantially reduced fuel-derived heat demands via internal heat recovery, decreasing to around 1.89 MWh/t-diesel for SOEC. Furthermore, internally recovered heat in the DAC system (2.27 MWh/t-diesel) is used to drive a Rankine cycle, generating electricity that partially offsets DAC and ASU power consumption.

In summary, the heat-integrated configuration enables the redistribution of energy flows, which lowers external fuel and electricity input, increases energy self-sufficiency, and frees up renewable electricity capacity, especially for high-demand units like the SOEC. This demonstrates the critical role of thermal integration in improving energy efficiency and decarbonization performance of synthetic fuel systems.

These results provide quantitative evidence supporting the system’s energy efficiency under integrated operation. Compared to the baseline configuration, heat integration reduces the system’s net external heat demand from 11.1 MWh/t-diesel to 3.6 MWh/t-diesel, a reduction of 67%, while offsetting 5% of total electricity requirements through internal recovery (Table 6). This internal reuse of thermal and electrical energy reflects a substantial gain in process-level efficiency. Additionally, the Sankey diagrams in Fig. 7 visualize the redistribution of energy streams, illustrating how recovered heat from the FT reactor, SOEC burner, and calciner displaces fuel-based heating and lowers the burden on renewable electricity sources. The increased availability of internal energy for high-demand units like the SOEC (from 3.1 MWh/t-diesel to 8.6 MWh/t-diesel of heat recovery) exemplifies how integration enhances self-sufficiency and reduces reliance on external utilities. Altogether, these results substantiate the claim that integrated thermal management leads to a significantly more energy-efficient process design.

To quantify the overall energy efficiency of the integrated DAC–SOEC–FT system, a process-level energy efficiency was defined as the ratio of the chemical energy stored in the synthetic diesel product to the total external energy input (electricity and net external heat):

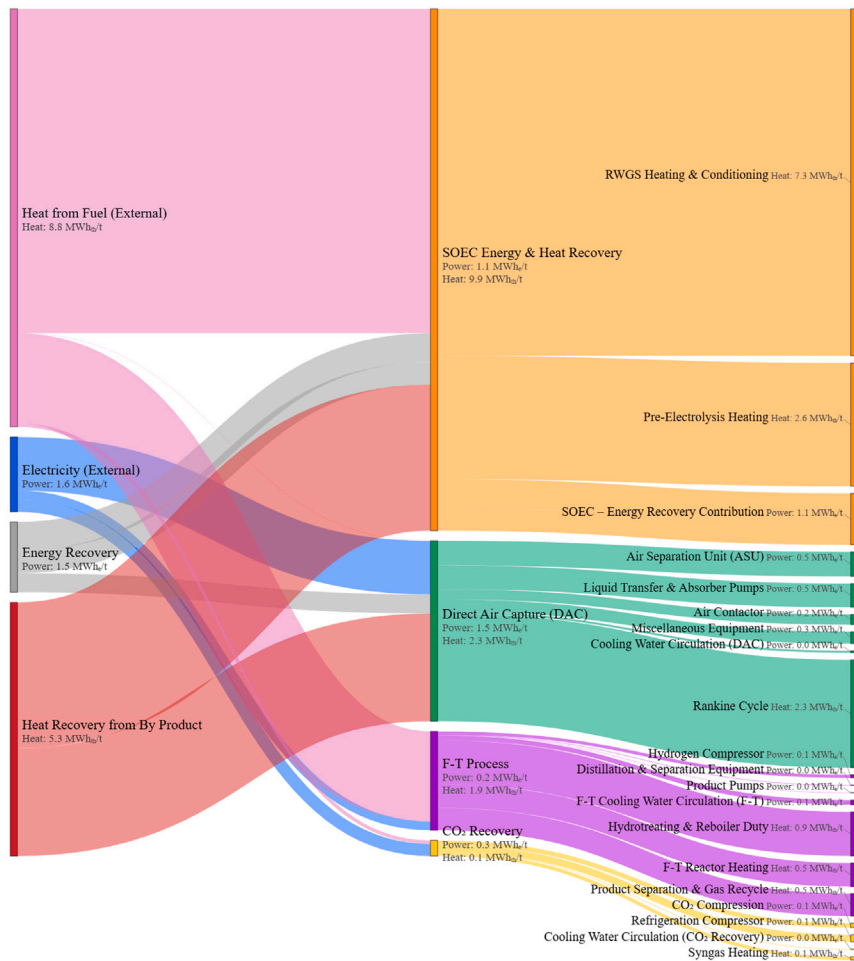
$$\eta_{\text{energy}} = \frac{\dot{m}_{\text{diesel}} \cdot \text{HHV}_{\text{diesel}}}{\dot{E}_{\text{el}} + \dot{E}_{\text{heat}}} \quad (32)$$

where  $\dot{m}_{\text{diesel}}$  is the diesel production rate,  $\text{HHV}_{\text{diesel}}$  is the higher heating value of diesel, and  $\dot{E}_{\text{el}}$  and  $\dot{E}_{\text{heat}}$  represent the total external electricity and heat inputs, respectively.

Assuming a diesel higher heating value of 11.8 MWh/t [121], and a plant capacity of 79.8 t/h of diesel, the energy output of the fuel corresponds to approximately 944 MWh/h. Under heat-integrated operation, the combined external energy input amounts to 35.0 MWh/t-diesel (31.4 MWh/t of electricity and 3.6 MWh/t of net heat), yielding an overall system energy efficiency of approximately 34%.

This metric reflects a process-level energy performance rather than a thermodynamic efficiency and is consistent with reported ranges for DAC-based power-to-liquids fuel pathways [122].

(a) DAC-SOEC-FT (Diesel) — without heat integration (WOHI)



(b) DAC-SOEC-FT (Diesel) — with heat integration (WHI)

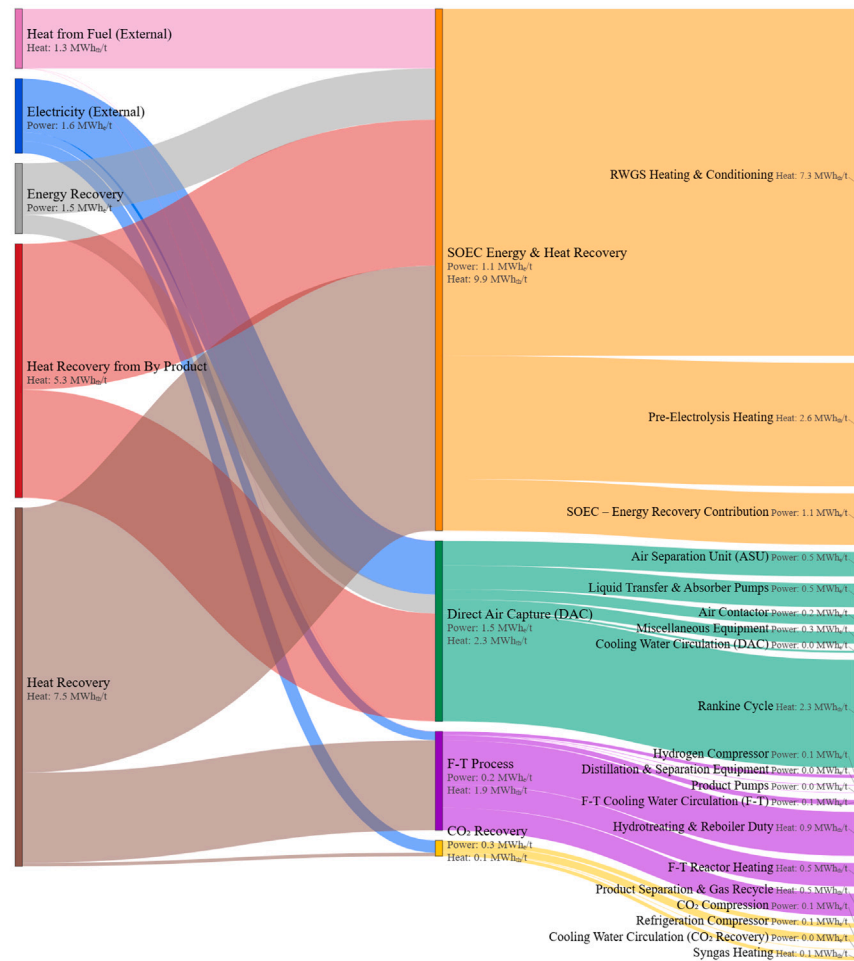
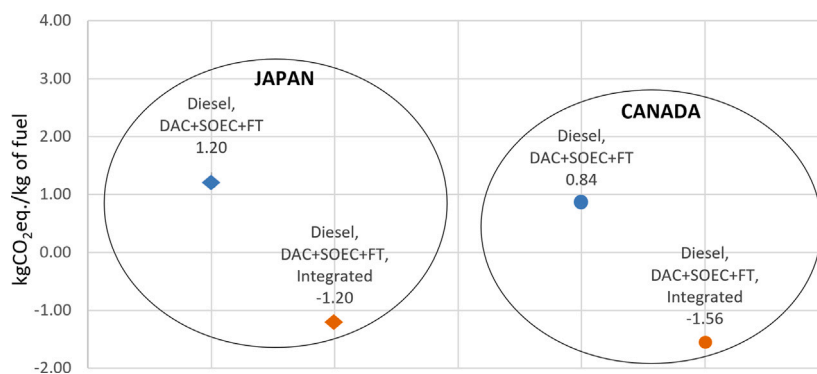


Fig. 7. Sankey comparison for DAC-SOEC-FT (diesel): (a) without heat integration; (b) with heat integration.

**Table 6**  
Electricity and heat consumption per ton of diesel (MWh/t) by process unit (without vs with heat integration)

Process	Electricity		Heat			
	Net electricity (MWh/t)	Electricity offset (%)	Net heat to utilities (MWh/t)		Heat recovery (%)	
			Without integration	With integration	Without integration	With integration
DAC	1.13	26	2.27	2.27	50	50
SOEC	29.82	4	6.82	1.25	31	87
CO <sub>2</sub> Recovery	0.26	0	0.08	0.00	0	100
FT process	0.19	0	2.03	0.14	0	93
<b>Total</b>	<b>31.40</b>	<b>5</b>	<b>11.20</b>	<b>3.66</b>	<b>32</b>	<b>78</b>

**Notes.** All energy values are reported in MWh per ton of diesel produced. Net heat to utilities refers to the external thermal energy required after internal recovery. Electricity offset is the share of a unit's electric load supplied internally. "Without integration" includes only by-product heat use; "With integration" includes both by-product and cross-unit heat recovery.



**Fig. 8.** Cradle-to-gate CO<sub>2</sub> emissions of DAC-derived synthetic diesel under integrated and non-integrated configurations in Japan and Canada.

The cradle-to-gate CO<sub>2</sub> emissions for DAC-derived synthetic diesel are compared across integrated and non-integrated configurations in Fig. 8. Results are shown for both Japan and Canada. In Japan, the non-integrated configuration yields 1.20 kg CO<sub>2</sub>-eq/kg-diesel, while the integrated configuration achieves cradle-to-gate net-negative emissions of -1.20 kg CO<sub>2</sub>-eq/kg-diesel. For Canada, emissions similarly decrease from 0.84 kg-CO<sub>2</sub>eq/kg-diesel to -1.56 kg CO<sub>2</sub>-eq/kg-diesel under integration. For context, the direct combustion of conventional fossil diesel emits approximately 3.19 kg CO<sub>2</sub>-eq/kg-diesel [123]. While this represents use-phase emissions only, it provides a benchmark for interpreting the magnitude of the cradle-to-gate carbon footprints obtained for the Japan and Canada cases.

For this comparison, we assume that the methane combusted in both Japan and Canada possesses identical chemical composition and calorific value, and thus apply a consistent emission intensity factor for methane combustion across both countries. In contrast, upstream emission intensities for inputs such as electricity and water are regionally differentiated, reflecting local supply chain and generation characteristics.

These negative cradle-to-gate values reflect the fact that, within the system boundary, more CO<sub>2</sub> is captured from the atmosphere than is emitted in the upstream energy supply and process operations. This outcome highlights how tight integration of DAC with downstream SOEC and FT synthesis, through heat recovery, internal energy reuse, and by-product valorization, can enable not only low-carbon but net-negative synthetic diesel production up to the refinery gate. The results also underline the importance of regional energy mix, as locations with cleaner grids (e.g., Canada) allow the integrated system to maximize its net-removal potential.

A simulation-based screening of variable operating costs (utilities and raw materials) was conducted for the integrated DAC-SOEC-FT diesel system under steady-state operation. The analysis considers grid electricity, renewable electricity supplied to the SOEC (solar in Japan and hydropower in Canada), methane fuel, and minor raw-material inputs (KOH and CaCO<sub>3</sub>). Representative regional energy prices were

applied for Japan and Canada to reflect differences in electricity supply and externally sourced methane fuel [124–126]. As shown in Fig. 9, heat integration lowers total variable OPEX by 21% in Japan and 6% in Canada through reduced methane consumption, while externally supplied electricity for SOEC operation remains the dominant cost contributor (> 80%). The smaller relative OPEX reduction in Canada reflects its substantially lower methane price, which limits the economic benefit of fuel savings from heat integration.

In addition to heat recovery, internal utilization of FT byproduct streams for heat and power generation is adopted as an energy-integration strategy to reduce reliance on externally supplied utilities and associated upstream emissions. While this reduces external utility demand, selling or upgrading these byproducts could improve economic performance by generating additional revenue. The present configuration therefore reflects an explicit trade-off, prioritizing minimization of external energy inputs and cradle-to-gate emissions over short-term economic optimization.

For context, the operating cost of conventional petroleum diesel production (excluding crude oil costs) is typically reported in the range of 20–65 USD/t-diesel, depending on refinery configuration and allocation methodology [127–129]. However, this value reflects only the refining stage of an already energy-dense fossil resource. In contrast, the integrated DAC-SOEC-FT system evaluated here involves both carbon capture from air and electrochemical hydrogen production, two energy-intensive processes necessary to achieve net-zero or carbon-negative liquid fuel pathways. The estimated utility and raw-material-based OPEX (1585–2789 USD/t-diesel) thus reflects the cost of atmospheric CO<sub>2</sub> fixation and synthetic fuel synthesis, not simply hydrocarbon processing. Rather than serving as a direct cost benchmark, this value offers a reference for understanding the operational expenses associated with e-fuel systems, particularly under current energy price conditions and technology maturity levels. This screening is limited to fixed operating expenses (e.g., labor, maintenance, and overheads) and all capital-related charges and should therefore be interpreted as a

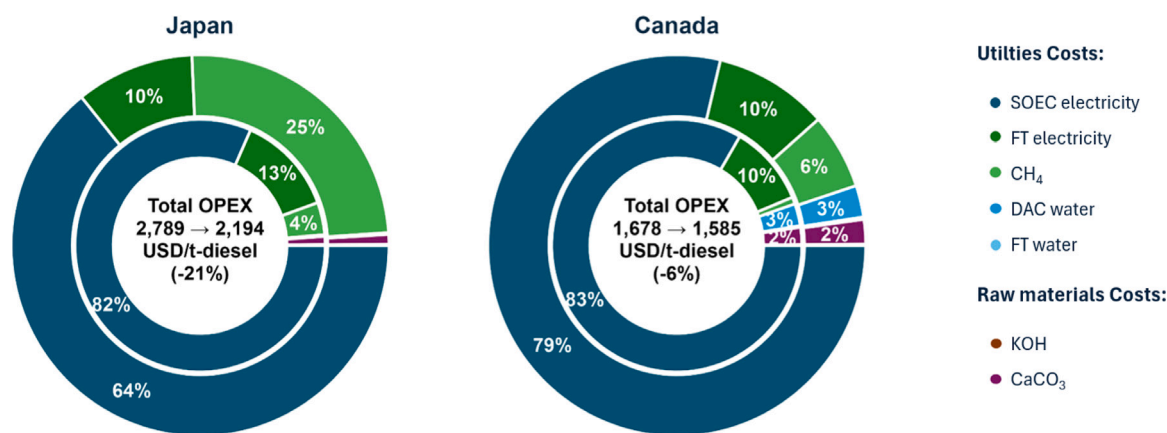


**Fig. 9.** Breakdown of utility and raw-material operating expenditure (OPEX) for DAC-SOEC-FT diesel production in Japan and Canada. The outer and inner rings represent configurations without heat integration (WOHI) and with heat integration (WHI), respectively. Center values indicate total variable OPEX in USD/t-diesel and the percentage reduction achieved through heat integration.

comparative indicator of energy-driven variable OPEX. A comprehensive economic assessment would additionally require consideration of capital expenditure and fixed operating costs.

## 5. Conclusions

The integration of Direct Air Capture (DAC) with co-electrolysis (SOEC) and Fischer-Tropsch (FT) synthesis for e-diesel production offers substantial performance advantages in both energy efficiency and cradle-to-gate CO<sub>2</sub> emissions. Simulation results show that tight coupling of these subsystems enables a high degree of internal energy recovery that significantly reduces external utility requirements. For instance, system-wide heat recovery increases from 32% in the non-integrated case to 78% with integration (Table 6), while internal electricity generation offsets up to 26% of DAC power demand. These benefits are visually reinforced by the Sankey diagrams, which highlight the shift in thermal load from fossil-derived heat toward internally recycled by-product energy streams.

Crucially, this integrated design achieves net-negative cradle-to-gate emissions, i.e., it removes more CO<sub>2</sub> from the atmosphere than it emits during fuel synthesis. In Canada and Japan, the integrated configuration yields -1.20 kg-CO<sub>2</sub>eq/kg-diesel and -1.56 kg-CO<sub>2</sub>eq/kg-diesel, respectively, driven by improved thermal coupling and better utilization of region-specific electricity mixes.

A key innovation in this configuration is the valorization of FT by-products, notably naphtha, gasoline, and purge gas, as internal fuel for the DAC calciner. These are carbon-neutral from a system accounting perspective, since their combustion releases previously captured biogenic or atmospheric CO<sub>2</sub>, avoiding additional emissions burdens. This closed-loop fuel strategy eliminates the need for external fossil-derived heat, further lowering the system's carbon intensity.

Despite these advantages, the SOEC unit remains the dominant electricity consumer, accounting for over 95% of the system's power demand. While heat integration reduces auxiliary loads and increases available energy for electrolysis pre-heating, the absolute renewable electricity requirement for SOEC remains a critical challenge for large-scale deployment. Nonetheless, the presented results demonstrate that high-efficiency integration can help ease this burden and improve the feasibility of net-negative fuel production.

Overall, this study highlights that deep integration of DAC, SOEC, and FT technologies enables strong synergistic behavior, with cascading benefits in energy reuse, emissions performance, and process flexibility. These findings underscore the importance of holistic system design in advancing sustainable, carbon-negative fuels for hard-to-decarbonize sectors such as aviation, shipping, and heavy transport.

## CRediT authorship contribution statement

**Alexander Guzman-Urbina:** Writing – review & editing, Writing – original draft, Visualization, Validation, Software, Methodology, Investigation, Formal analysis, Data curation, Conceptualization. **Tantiwatthanaphanich Thanapan:** Writing – review & editing, Writing – original draft, Visualization, Software, Methodology, Investigation, Formal analysis. **Jubil Joy:** Writing – original draft, Methodology, Investigation, Formal analysis, Data curation. **Karina Anaya:** Writing – original draft, Methodology, Investigation, Formal analysis. **Jalil Shadbahr:** Writing – review & editing, Writing – original draft, Supervision, Resources, Formal analysis. **Amit Kumar:** Writing – original draft, Supervision, Resources, Conceptualization. **Giovanna Gonzales-Calienes:** Resources, Funding acquisition. **Shinichirou Morimoto:** Writing – original draft, Supervision, Project administration, Funding acquisition, Conceptualization.

## Declaration of competing interest

The authors declare that they have no known competing financial interests or personal relationships that could have appeared to influence the work reported in this paper.

## Acknowledgments

This work was supported by the New Energy and Industrial Technology Development Organization (NEDO) of Japan under the in-house projects in E-fuels, and by the National Program Office (NPO) of the National Research Council Canada (NRC) under the Materials for Clean Fuels (MCF) Challenge Program (project number MCF-135-1).

## Appendix A. Supplementary data

Supplementary material related to this article can be found online at <https://doi.org/10.1016/j.jcou.2026.103319>.

## Data availability

Data will be made available on request.

## References

- [1] IPCC, Climate change 2021: The physical science basis. Summary for policy-makers, 2021, URL: <https://www.ipcc.ch/report/ar6/wg1/>. Working Group I Contribution to the Sixth Assessment Report of the Intergovernmental Panel on Climate Change. Intergovernmental Panel on Climate Change.
- [2] J. Rockström, et al., A safe operating space for humanity, *Nature* 461 (7263) (2009) 472–475, <http://dx.doi.org/10.1038/461472a>.
- [3] UNFCCC, The Paris agreement, 2015, <https://unfccc.int/process-and-meetings/the-paris-agreement/the-paris-agreement>.
- [4] International Energy Agency, Net zero by 2050: A roadmap for the global energy sector, 2021, <https://www.iea.org/reports/net-zero-by-2050>.
- [5] N. Stern, *The Economics of Climate Change: The Stern Review*, Cambridge University Press, 2007.
- [6] International Energy Agency, Net zero roadmap: A global pathway to keep the 1.5°C goal in reach, 2023, <https://www.iea.org/reports/net-zero-roadmap-a-global-pathway-to-keep-the-15-c-goal-in-reach-2023-update>.
- [7] A. Kumar, A.K. Tiwari, D. Milani, Decarbonizing hard-to-abate heavy industries: Current status and pathways towards net-zero future, *Process. Saf. Environ. Prot.* (2024).
- [8] S.J. Davis, N.S. Lewis, M. Shaner, S. Aggarwal, D. Arent, I.L. Azevedo, S.M. Benson, T. Bradley, J. Brouwer, Y.-M. Chiang, et al., Net-zero emissions energy systems, *Science* 360 (6396) (2018) eaas9793, <http://dx.doi.org/10.1126/science.aas97>.
- [9] S.Y. Searle, C.J. Malins, Waste and residue availability for advanced biofuel production in EU member states, *Biomass Bioenergy* 89 (2016) 2–10, <http://dx.doi.org/10.1016/j.biombioe.2016.01.008>.
- [10] M. Fasihi, O. Efimova, C. Breyer, Techno-economic assessment of CO2 direct air capture plants, *J. Clean. Prod.* 224 (2019) 957–980, <http://dx.doi.org/10.1016/j.jclepro.2019.03.086>.
- [11] S. Brynolf, M. Taljegard, M. Grahn, J. Hansson, Electrofuels for the transport sector: A review of production costs, *Renew. Sustain. Energy Rev.* 81 (2018) 1887–1905, <http://dx.doi.org/10.1016/j.rser.2017.05.288>.
- [12] U.S. Department of Energy, Alternative Fuels Data Center, Synthetic fuels, 2024, [https://afdc.energy.gov/fuels/emerging\\_synthetic.html](https://afdc.energy.gov/fuels/emerging_synthetic.html).
- [13] N. Mac Dowell, P.S. Fennell, N. Shah, G.C. Maitland, The role of CO2 capture and utilization in mitigating climate change, *Nat. Clim. Chang.* 7 (4) (2017) 243–249, <http://dx.doi.org/10.1038/nclimate3231>.
- [14] P. Warren, M. Frazer, N. Greenwood, Role of climate finance beyond renewables: hard-to-abate sectors, *Energy Rep.* 10 (2023) 3519–3531, <http://dx.doi.org/10.1016/j.egyr.2023.10.021>.
- [15] S. Horvath, M. Fasihi, C. Breyer, Techno-economic analysis of a decarbonized shipping sector: Technology suggestions for a fleet in 2030 and 2040, *Energy Convers. Manage.* 164 (2018) 230–241, <http://dx.doi.org/10.1016/j.enconman.2018.02.098>.
- [16] J. Kim, Y. Yuan, Y. Ren, B.A. McCool, R.P. Lively, M.J. Realf, Carbon and oxygen recycling strategies in CO2-to-sustainable synthetic fuel production: Recycling route, techno-economics and carbon intensity, *Energy Convers. Manage.* 319 (2024) 118877, <http://dx.doi.org/10.1016/j.enconman.2024.118877>.
- [17] F.O. Ochedi, J. Yu, H. Yu, Y. Liu, A. Hussain, Carbon dioxide capture using liquid absorption methods: a review, *Environ. Chem. Lett.* 19 (2021) 77–109, <http://dx.doi.org/10.1007/s10311-020-01093-8>.
- [18] G. Leonzio, P.S. Fennell, N. Shah, A comparative study of different sorbents in the context of direct air capture (DAC): evaluation of key performance indicators and comparisons, *Appl. Sci.* 12 (5) (2022) 2618, <http://dx.doi.org/10.3390/app12052618>.
- [19] S.-Y. Kim, A. Sarswat, S. Cho, M. Song, J. Kim, M.J. Realf, D.S. Sholl, R.P. Lively, Near-cryogenic direct air capture using adsorbents, *Energy Environ. Sci.* 18 (15) (2025) 7427–7439, <http://dx.doi.org/10.1039/D5EE01473E>.
- [20] IEA, World Energy Outlook 2024, IEA, Paris, 2024, Licence: CC BY 4.0 (report); CC BY NC SA 4.0 (Annex A). <https://www.iea.org/reports/world-energy-outlook-2024>.
- [21] IEA, Net Zero Roadmap: A Global Pathway to Keep the 1.5 % C Goal in Reach, IEA, Paris, 2023, <https://www.iea.org/reports/net-zero-roadmap-a-global-pathway-to-keep-the-15-c-goal-in-reach>. Licence: CC BY 4.0.
- [22] P. Jaramillo, S. Kahn Ribeiro, P. Newman, S. Dhar, O. Diemuodeke, T. Kajino, D. Lee, S. Nugroho, X. Ou, A. Stromman, J. Whitehead, Transport, in: P. Shukla, J. Skea, R. Slade, A. Al Khourdajie, R. van Diemen, D. McCollum, M. Pathak, S. Some, P. Vyas, R. Fradera, M. Belkacemi, A. Hasija, G. Lisboa, S. Luz, J. Malley (Eds.), *Climate Change 2022: Mitigation of Climate Change. Contribution of Working Group III to the Sixth Assessment Report of the Intergovernmental Panel on Climate Change*, Cambridge University Press, Cambridge, UK and New York, NY, USA, 2022, <http://dx.doi.org/10.1017/9781009157926.012>.
- [23] I.A. Bashmakov, L.J. Nilsson, A. Acquaye, C. Bataille, J.M. Cullen, S. de la Rue du Can, M. Fischedick, Y. Geng, K. Tanaka, Industry, in: P.R. Shukla, J. Skea, R. Slade, A. Al Khourdajie, R. van Diemen, D. McCollum, M. Pathak, S. Some, P. Vyas, R. Fradera, M. Belkacemi, A. Hasija, G. Lisboa, S. Luz, J. Malley (Eds.), *Climate Change 2022: Mitigation of Climate Change. Contribution of Working Group III to the Sixth Assessment Report of the Intergovernmental Panel on Climate Change*, Cambridge University Press, Cambridge, UK and New York, NY, USA, 2022, <http://dx.doi.org/10.1017/9781009157926.013>.
- [24] F. Creutzig, P. Jochem, O.Y. Edelenbosch, L. Mattauch, J. Minx, et al., Transport: A roadblock to climate change mitigation? Urban mobility solutions foster climate mitigation, *Science* 350 (6263) (2015) 911–912, <http://dx.doi.org/10.1126/science.aac8033>.
- [25] M. Sendi, M. Bui, N. Mac Dowell, P. Fennell, Geospatial techno-economic and environmental assessment of different energy options for solid sorbent direct air capture, *Cell Rep. Sustain.* 1 (8) (2024) 100151, <http://dx.doi.org/10.1016/j.crsus.2024.100151>, URL: <https://www.sciencedirect.com/science/article/pii/S2949790624002374>.
- [26] D.W. Keith, G. Holmes, D. St. Angelo, K. Heidele, A process for capturing CO2 from the atmosphere, *Joule* 2 (8) (2018) 1573–1594, <http://dx.doi.org/10.1016/j.joule.2018.05.006>.
- [27] S. Deutz, A. Bardow, Life-cycle assessment of an industrial direct air capture process based on temperature–vacuum swing adsorption, *Nat. Energy* 6 (2021) 203–213, <http://dx.doi.org/10.1038/s41560-020-00771-9>.
- [28] S. Morimoto, N. Kitagawa, F. Bensebaa, A. Kumar, S. Kataoka, S. Taniguchi, Scenario assessment of introducing carbon utilization and carbon removal technologies considering future technological transition based on renewable energy and direct air capture, *J. Clean. Prod.* 402 (2023) 136763, <http://dx.doi.org/10.1016/j.jclepro.2023.136763>.
- [29] A. Guzman-Urbina, N. Kitagawa, D. Richards, E. Kourogi, S. Morimoto, Advancing e-methanol systems via direct air carbon capture, CO2 hydrogenation, and hydrothermal co-electrolysis, *J. Clean. Prod.* 528 (2025) 146699, <http://dx.doi.org/10.1016/j.jclepro.2025.146699>.
- [30] A.S. Emam, M.O. Hamdan, B.A. Abu-Nabah, E. Elnajjar, A review on recent trends, challenges, and innovations in alkaline water electrolysis, *Int. J. Hydrog. Energy* 64 (2024) 599–625, <http://dx.doi.org/10.1016/j.ijhydene.2024.03.238>.
- [31] J. Brauns, T. Turek, Alkaline water electrolysis powered by renewable energy: A review, *Processes* 8 (2) (2020) <http://dx.doi.org/10.3390/pr8020248>.
- [32] A. Buttler, H. Spliethoff, Current status of water electrolysis for energy storage, grid balancing and sector coupling via power-to-gas and power-to-liquids: A review, *Renew. Sustain. Energy Rev.* 82 (2018) 2440–2454, <http://dx.doi.org/10.1016/j.rser.2017.09.003>.
- [33] A. Vedrtam, K. Kalauni, R. Pahwa, A review of water electrolysis technologies with insights into optimization and numerical simulations, *Int. J. Hydrog. Energy* 140 (2025) 694–727, <http://dx.doi.org/10.1016/j.ijhydene.2025.05.295>.
- [34] L. Yang, P. Xie, R. Zhang, Y. Cheng, B. Cai, R. Wang, HIES: Cases for hydrogen energy and I-Energy, *Int. J. Hydrog. Energy* 44 (56) (2019) 29785–29804, <http://dx.doi.org/10.1016/j.ijhydene.2019.03.056>.
- [35] M. Kisti, B. Huner, A. Albadwi, E. Ozdogan, I.N. Uzgoren, S. Uysal, M. Conaggasi, Y.O. Suzen, N. Demir, M.F. Kaya, Recent advances in polymer electrolyte membrane water electrolyzer stack development studies: A review, *ACS Omega* 10 (10) (2025) 9824–9853, <http://dx.doi.org/10.1021/acsomega.4c10147>.
- [36] S.A. Grigoriev, A.A. Kalinnikov, Mathematical modeling and experimental study of the performance of PEM water electrolysis cell with different loadings of platinum metals in electrocatalytic layers, *Int. J. Hydrog. Energy* 42 (3) (2017) 1590–1597, <http://dx.doi.org/10.1016/j.ijhydene.2016.09.058>.
- [37] T. Wang, X. Cao, L. Jiao, PEM water electrolysis for hydrogen production: fundamentals, advances, and prospects, *Carbon Neutrality* 1 (1) (2022) 21, <http://dx.doi.org/10.1007/s43979-022-00022-8>.
- [38] J. Kim, H. Lee, B. Lee, J. Kim, H. Oh, I.-B. Lee, Y.-S. Yoon, H. Lim, An integrative process of blast furnace and SOEC for hydrogen utilization: Techno-economic and environmental impact assessment, *Energy Convers. Manage.* 250 (2021) 114922, <http://dx.doi.org/10.1016/j.enconman.2021.114922>.
- [39] S. Zong, X. Zhao, L.L. Jewell, Y. Zhang, X. Liu, Advances and challenges with SOEC high temperature co-electrolysis of CO2/H2O: Materials development and technological design, *Carbon Capture Sci. Technol.* 12 (2024) 100234, <http://dx.doi.org/10.1016/j.ccst.2024.100234>.
- [40] J. Chen, X. Gao, X. Chen, Z. Zhen, Y. Chen, X. Zeng, L. Cui, Recent advances of perovskite oxide-based cathodes in solid oxide electrolysis cells for CO2 electroreduction, *Mater. Today Phys.* 38 (2023) 101237, <http://dx.doi.org/10.1016/j.mtphys.2023.101237>.
- [41] G. Sassone, O. Celikkilek, M. Hubert, K. Develos-Bagarinao, T. David, L. Guetaz, I. Martin, J. Villanova, A. Benayad, L. Rorato, et al., Effect of the operating temperature on the degradation of solid oxide electrolysis cells, *J. Power Sources* 605 (2024) 234541, <http://dx.doi.org/10.1016/j.jpowsour.2024.234541>.
- [42] J. Du, W. Yang, L. Xu, L. Bei, S. Lei, W. Li, H. Liu, B. Wang, L. Sun, Review on post-combustion CO2 capture by amine blended solvents and aqueous ammonia, *Chem. Eng. J.* 488 (2024) 150954, <http://dx.doi.org/10.1016/j.cej.2024.150954>.
- [43] X. He, H. He, F. Barzagli, M.W. Amer, C. Li, R. Zhang, Analysis of the energy consumption in solvent regeneration processes using binary amine blends for CO2 capture, *Energy* 270 (2023) 126903, <http://dx.doi.org/10.1016/j.energy.2023.126903>.
- [44] G. Fytianos, S. Ucar, A. Grimstvedt, A. Hyldebakk, H.F. Svendsen, H.K. Knuutila, Corrosion and degradation in MEA based post-combustion CO2 capture, *Int. J. Greenh. Gas Control.* 46 (2016) 48–56, <http://dx.doi.org/10.1016/j.ijggc.2015.12.028>.

- [45] P. Gkotsis, P. Kougiyas, M. Mitrakas, A. Zouboulis, Biogas upgrading technologies – recent advances in membrane-based processes, *Int. J. Hydrog. Energy* 48 (10) (2023) 3965–3993, <http://dx.doi.org/10.1016/j.ijhydene.2022.10.228>.
- [46] M. Kárászová, B. Zach, Z. Petrusová, V. Červenka, M. Bobák, M. Šyc, P. Izák, Post-combustion carbon capture by membrane separation, review, *Sep. Purif. Technol.* 238 (2020) 116448, <http://dx.doi.org/10.1016/j.seppur.2019.116448>.
- [47] H. Zentou, B. Hoque, M.A. Abdalla, A.F. Saber, O.Y. Abdelaziz, M. Aliyu, A.M. Alkhedhair, A.J. Alabduly, M.M. Abdelnaby, Recent advances and challenges in solid sorbents for CO<sub>2</sub> capture, *Carbon Capture Sci. Technol.* (2025) 100386, <http://dx.doi.org/10.1016/j.ccsst.2025.100386>.
- [48] A. Al-Mamoori, A. Krishnamurthy, A.A. Rownaghi, F. Rezaei, Carbon capture and utilization update, *Energy Technol.* 5 (6) (2017) 834–849, <http://dx.doi.org/10.1002/ente.201600747>.
- [49] K.H. Smith, H.E. Ashkanani, B.I. Morsi, N.S. Siefert, Physical solvents and techno-economic analysis for pre-combustion CO<sub>2</sub> capture: A review, *Int. J. Greenh. Gas Control.* 118 (2022) 103694, <http://dx.doi.org/10.1016/j.jggc.2022.103694>.
- [50] A. Dave, B. Pathak, M. Dave, S. Rezvani, Y. Huang, N. Hewitt, Process design of CO<sub>2</sub> desorption from physical solvent di-methyl-ether of poly-ethylene-glycol, *Mater. Sci. Energy Technol.* 3 (2020) 209–217, <http://dx.doi.org/10.1016/j.mset.2019.09.005>.
- [51] J.G. Speight, Chapter 8 - hydrocarbons from synthesis gas, in: *Handbook of Industrial Hydrocarbon Processes*, second ed., 2020, pp. 343–386.
- [52] D.H. Y. Yao, D. Glasser, The effect of CO<sub>2</sub> on a cobalt-based catalyst for low temperature Fischer–Tropsch synthesis, *Chem. Eng. J.* 193–194 (2012) 318–327, <http://dx.doi.org/10.1016/j.cej.2012.04.045>.
- [53] P. Kaiser, R.B. Unde, C. Kern, A. Jess, Production of liquid hydrocarbons with CO<sub>2</sub> as carbon source based on reverse water-gas shift and Fischer–Tropsch synthesis, *Chem. Ing. Tech.* 85 (4) (2013) 489–499, <http://dx.doi.org/10.1002/cite.201200179>.
- [54] J. Wenstrup, G.R. Pesch, J. Thöming, Dynamic operation of Fischer–Tropsch reactors for power-to-liquid concepts: A review, *Renew. Sustain. Energy Rev.* 162 (2022) 112454, <http://dx.doi.org/10.1016/j.rser.2022.112454>.
- [55] H. Eilers, M.I. González, G. Schaub, Lab-scale experimental studies of Fischer–Tropsch kinetics in a three-phase slurry reactor under transient reaction conditions, *Catal. Today* 275 (2016) 164–171, <http://dx.doi.org/10.1016/j.cattod.2015.11.011>.
- [56] J. Shadbahr, C.A. Peeples, E. Pahija, C. Panaritis, D.C. Boffito, G. Patience, F. Bensebaa, Sustainability assessment of catalyst design on CO<sub>2</sub>-derived fuel production, *Renew. Sustain. Energy Rev.* 208 (2025) 115011, <http://dx.doi.org/10.1016/j.rser.2024.115011>.
- [57] A. Keunecke, M. Dossow, V. Dieterich, H. Spliethoff, S. Fendt, Insights into Fischer–Tropsch catalysis: current perspectives, mechanisms, and emerging trends in energy research, *Front. Energy Res.* 12 (2024) 1–11, <http://dx.doi.org/10.3389/fenrg.2024.1344179>.
- [58] F. Bisotti, K.A. Hoff, A. Mathisen, J. Hovland, Direct air capture (DAC) deployment: A review of the industrial deployment, *Chem. Eng. Sci.* 283 (2024) 119416, <http://dx.doi.org/10.1016/j.ces.2023.119416>.
- [59] S.E. Wolf, F.E. Winterhalter, V. Vibhu, L.B. de Haart, O. Guillon, R.-A. Eichel, N.H. Menzler, Solid oxide electrolysis cells—current material development and industrial application, *J. Mater. Chem. A* 11 (34) (2023) 17977–18028, <http://dx.doi.org/10.1039/D3TA02161K>.
- [60] C.M. Liu, N.K. Sandhu, S.T. McCoy, J.A. Bergerson, A life cycle assessment of greenhouse gas emissions from direct air capture and Fischer–Tropsch fuel production, *Sustain. Energy Fuels* 4 (2020) 3129–3142, <http://dx.doi.org/10.1039/C9SE00479C>.
- [61] X. Zhang, C. Bauer, C. Mutel, K. Volkart, Life cycle assessment of power-to-gas: Approaches, system variations and their environmental implications, *Appl. Energy* 190 (2017) 326–338, <http://dx.doi.org/10.1016/j.apenergy.2016.12.098>.
- [62] R. Cuéllar-Franca, A. Azapagic, Carbon capture, storage and utilisation technologies: A critical analysis and comparison of their life cycle environmental impacts, *J. CO<sub>2</sub> Util.* 9 (2015) 82–102, <http://dx.doi.org/10.1016/j.jcou.2014.12.001>.
- [63] G. Garcia-Garcia, M. Fernandez, K. Armstrong, S. Woolass, P. Styring, Analytical review of life-cycle environmental impacts of carbon capture and utilization technologies, *ChemSusChem* 14 (2021) 995–1015, <http://dx.doi.org/10.1002/cssc.202002126>.
- [64] C. Hepburn, E. Adlen, J. Beddington, E. Carter, S. Fuss, N. Mac Dowell, J. Minx, P. Smith, C. Williams, The technological and economic prospects for CO<sub>2</sub> utilization and removal, *Nature* 575 (2019) 87–97, <http://dx.doi.org/10.1038/s41586-019-1681-6>.
- [65] J. Minx, W. Lamb, M. Callaghan, S. Fuss, J. Hilaire, F. Creutzg, T. Amann, T. Beringer, W. de Oliveira Garcia, J. Hartmann, T. Khanna, D. Lenzi, G. Luderer, G. Nemet, J. Rogelj, P. Smith, J. Vicente Vicente, J. Wilcox, M.d.M. Zamora Dominguez, Negative emissions - part 1: Research landscape and synthesis, *Environ. Res. Lett.* 13 (6) (2018) 063001, <http://dx.doi.org/10.1088/1748-9326/aabf9b>.
- [66] C. Shi, B. Labbaf, E. Mostafavi, N. Mahinpey, Methanol production from water electrolysis and tri-reforming: Process design and technical-economic analysis, *J. CO<sub>2</sub> Util.* 38 (2020) 241–251, <http://dx.doi.org/10.1016/j.jcou.2019.12.022>.
- [67] A. Tripodi, F. Conte, I. Rossetti, Carbon dioxide methanation: Design of a fully integrated plant, *Energy Fuels* 34 (2020) 7242–7256, <http://dx.doi.org/10.1021/acs.energyfuels.0c00580>.
- [68] I.J. Okeke, K. Sahoo, N. Kaliyan, S. Mani, Life cycle assessment of renewable diesel production via anaerobic digestion and Fischer–Tropsch synthesis from miscanthus grown in strip-mined soils, *J. Clean. Prod.* 249 (2020) 119358, <http://dx.doi.org/10.1016/j.jclepro.2019.119358>, URL: <https://www.sciencedirect.com/science/article/pii/S0959652619342283>.
- [69] T.K. Poddar, G.G. Zaines, S. Kar, D.M. Walker, T.R. Hawkins, Life cycle analysis of Fischer–Tropsch diesel produced by tri-reforming and Fischer–Tropsch synthesis (TriFITS) of landfill gas, *Environ. Sci. Technol.* 57 (48) (2023) 19602–19611, <http://dx.doi.org/10.1021/acs.est.3c02162>.
- [70] U.S. DOE., Best Practices for Life Cycle Assessment (LCA) of Direct Air Capture with Storage (DACs), Technical Report, U.S. Department of Energy, Office of Fossil Energy and Carbon Management, 2022, URL: <https://www.energy.gov/fecm/best-practices-LCA-DACS>.
- [71] T. Langhorst, et al., Techno-Economic Assessment and Life Cycle Assessment Guidelines for CO<sub>2</sub> Utilization, Global CO<sub>2</sub> Initiative, 2020, <http://dx.doi.org/10.7302/4190>, (Accessed 29 May 2025).
- [72] IEA, Greenhouse Gas Accounting for CO<sub>2</sub> Capture and Utilisation (CCU) Technologies – Greenhouse Gas Accounting Guidelines for CCU, IEAGHG Technical Review 2018-TR01b, 2018, <https://publications.ieaghg.org/technicalreports/2018TR1a>.
- [73] W. Becker, R. Braun, M. Penev, M. Melaina, Production of fischer-tropsch liquid fuels from high temperature solid oxide co-electrolysis units, *Energy* 47 (2012) 99–115, <http://dx.doi.org/10.1016/j.energy.2012.08.047>.
- [74] A. Ghorbani, A. Gharehghani, J. Saray, A. Andwari, T. Borhani, Integration of direct air capture with Allam cycle: Innovative pathway in negative emission technologies, *Energy Convers. Manage.* 332 (2025) 119746, <http://dx.doi.org/10.1016/j.enconman.2025.119746>.
- [75] J. Joy, R. Singla, K. Chowdhury, Safe design of liquid oxygen plant that absorbs LNG cold energy and offsets supply disruption by injecting liquid nitrogen, *Sustain. Energy Technol. Assess.* 53 (2022) 102501, <http://dx.doi.org/10.1016/j.seta.2022.102501>.
- [76] A. Kamkeng, M. Wang, Technical analysis of the modified Fischer–Tropsch synthesis process for direct CO<sub>2</sub> conversion into gasoline fuel: Performance improvement via ex-situ water removal, *Chem. Eng. J.* 462 (2023) 142048, <http://dx.doi.org/10.1016/j.cej.2023.142048>.
- [77] K. Im-orb, N. Visitdumrongkul, D. Saebae, Y. Patcharavorachot, A. Arpornwichanop, Flowsheet-based model and exergy analysis of solid oxide electrolysis cells for clean hydrogen production, *J. Clean. Prod.* 170 (2018) 1–13, <http://dx.doi.org/10.1016/j.jclepro.2017.09.127>.
- [78] J. Liang, Y. Wang, J. Zhu, M. Han, K. Sun, Z. Sun, Investigation on the reaction mechanism of solid oxide co-electrolysis with different inlet mixtures based on the comparison of CO<sub>2</sub> electrolysis and H<sub>2</sub>O electrolysis, *Energy Convers. Manage.* 277 (2023) 116621, <http://dx.doi.org/10.1016/j.enconman.2022.116621>.
- [79] D. Im, K. Roh, J. Kim, Y. Eom, J. Lee, Economic assessment and optimization of the Selexol process with novel additives, *Int. J. Greenh. Gas Control.* 42 (2015) 109–116, <http://dx.doi.org/10.1016/j.jggc.2015.08.001>.
- [80] G. Cinti, A. Baldinelli, A. Di Michele, U. Desideri, Integration of solid oxide electrolyzer and Fischer–Tropsch: A sustainable pathway for synthetic fuel, *Appl. Energy* 162 (2016) 308–320, <http://dx.doi.org/10.1016/j.apenergy.2015.10.053>.
- [81] S. Bube, N. Bullerdiek, S. Voß, M. Kaltschmitt, Kerosene production from power-based syngas – a technical comparison of the Fischer–Tropsch and methanol pathway, *Fuel* 366 (2024) 131269, <http://dx.doi.org/10.1016/j.fuel.2024.131269>.
- [82] Z. He, W. Zhao, G. Liu, Y. Qian, X. Lu, Effects of short chain aromatics in gasoline on GDI engine combustion and emissions, *Fuel* 297 (2021) 120725, <http://dx.doi.org/10.1016/j.fuel.2021.120725>.
- [83] Q. Kong, N. Shah, Development of an optimization-based framework for simultaneous process synthesis and heat integration, *Ind. Eng. Chem. Res.* 56 (2017) 5000–5013, <http://dx.doi.org/10.1021/acs.iecr.7b00549>.
- [84] Y. Zhao, H. Xue, X. Jin, B. Xiong, R. Liu, Y. Peng, et al., System level heat integration and efficiency analysis of hydrogen production process based on solid oxide electrolysis cells, *Int. J. Hydrog. Energy* 46 (2021) 38163–38174, <http://dx.doi.org/10.1016/j.ijhydene.2021.09.105>.
- [85] H. Holmes, M. Realf, R. Lively, Water management and heat integration in direct air capture systems, *Nat. Chem. Eng.* 1 (2024) 208–215, <http://dx.doi.org/10.1038/s44286-024-00032-6>.
- [86] M. Marchese, G. Buffo, M. Santarelli, A. Lanzini, CO<sub>2</sub> from direct air capture as carbon feedstock for Fischer–Tropsch chemicals and fuels: Energy and economic analysis, *J. CO<sub>2</sub> Util.* 46 (2021) 101487, <http://dx.doi.org/10.1016/j.jcou.2021.101487>.
- [87] E. Prats-Salvado, N. Monnerie, C. Sattler, Synergies between direct air capture technologies and solar thermochemical cycles in the production of methanol, *Energies* 14 (2021) 4818, <http://dx.doi.org/10.3390/en14164818>.

- [88] Z. Zolfaghari, A. Aslani, R. Zahedi, S. Kazzazi, Simulation of carbon dioxide direct air capture plant using potassium hydroxide aqueous solution: Energy optimization and CO<sub>2</sub> purity enhancement, *Energy Convers. Manag.* X 21 (2024) 100489, <http://dx.doi.org/10.1016/j.ecmx.2023.100489>.
- [89] D.W. Keith, G. Holmes, D. St. Angelo, K. Heidel, A process for capturing CO<sub>2</sub> from the atmosphere, *Joule* 2 (8) (2018) 1573–1594, <http://dx.doi.org/10.1016/j.joule.2018.05.006>, URL: <https://www.sciencedirect.com/science/article/pii/S2542435118302253>.
- [90] A. Kumar, A.K. Tiwari, D.U. Cearnaigh, Comparative analysis of benchmark and aeon blue technologies for sustainable efuel production: Integrating direct air capture and green hydrogen approaches, *Energy Convers. Manag.* 308 (2024) 118384, <http://dx.doi.org/10.1016/j.enconman.2024.118384>.
- [91] S. Divekar, A. Arya, A. Hanif, R. Chauhan, P. Gupta, A. Nanoti, et al., Recovery of hydrogen and carbon dioxide from hydrogen PSA tail gas by vacuum swing adsorption, *Sep. Purif. Technol.* 254 (2021) 117113, <http://dx.doi.org/10.1016/j.seppur.2020.117113>.
- [92] M. Luberti, H. Ahn, Review of polybed pressure swing adsorption for hydrogen purification, *Int. J. Hydrog. Energy* 47 (2022) 10911–10933, <http://dx.doi.org/10.1016/j.ijhydene.2022.01.147>.
- [93] Y. Redissi, C. Bouallou, Valorization of carbon dioxide by co-electrolysis of CO<sub>2</sub>/H<sub>2</sub>O at high temperature for syngas production, *Energy Procedia* 37 (2013) 6667–6678, <http://dx.doi.org/10.1016/j.egypro.2013.06.599>.
- [94] F. Vidal Vázquez, P. Pfeifer, J. Lehtonen, P. Piermartini, P. Simell, V. Alopaeus, Catalyst screening and kinetic modeling for CO production by high pressure and temperature reverse water gas shift for Fischer-Tropsch applications, *Ind. Eng. Chem. Res.* 56 (2017) 13262–13272, <http://dx.doi.org/10.1021/acs.iecr.7b01606>.
- [95] A. Hauch, K. Brodersen, M. Chen, M.B. Mogensen, Ni/YSZ electrodes structures optimized for increased electrolysis performance and durability, *Solid State Ion.* 293 (2016) 27–36, <http://dx.doi.org/10.1016/j.ssi.2016.06.003>.
- [96] P. Tyagi, *Thermochemistry*, first ed., Discovery Publishing Pvt. Ltd., New Delhi, 2006.
- [97] G. Zang, P. Sun, E.H. Delgado, V. Cappello, C. Ng, A. Elgowainy, The modeling of synfuel production process, 2022, URL: <https://publications.anl.gov/anlpubs/2022/05/175009.pdf>. (Accessed 20 April 2025).
- [98] F. Shi, *Reactor and Process Design in Sustainable Energy Technology*, Elsevier, 2014, <http://dx.doi.org/10.1016/B978-0-444-59566-9.00006-5>.
- [99] M.E. Dry, High quality diesel via the Fischer-Tropsch process - A review, *J. Chem. Technol. Biotechnol.* 77 (2002) 43–50, <http://dx.doi.org/10.1002/jctb.527>.
- [100] D. Leckel, Diesel production from Fischer-Tropsch: The past, the present, and new concepts, *Energy Fuels* 23 (2009) 2342–2358, <http://dx.doi.org/10.1021/ef900064c>.
- [101] D.S. Newsome, The water-gas shift reaction, *Catal. Rev.* 21 (1980) 275–318, <http://dx.doi.org/10.1080/03602458008067535>.
- [102] C. Ndimande, *Ideal Hydrocracking Catalysts for the Conversion Of FT Wax to Diesel* (Ph.D. thesis), University of Cape Town, 2014.
- [103] M. Marchese, E. Giglio, M. Santarelli, A. Lanzini, Energy performance of power-to-liquid applications integrating biogas upgrading, reverse water gas shift, solid oxide electrolysis and Fischer-Tropsch technologies, *Energy Convers. Manag.* X 6 (2020) 100041, <http://dx.doi.org/10.1016/j.ecmx.2020.100041>.
- [104] M. Samavati, M. Santarelli, A. Martin, V. Nemanova, Thermodynamic and economy analysis of solid oxide electrolyser system for syngas production, *Energy* 122 (2017) 37–49, <http://dx.doi.org/10.1016/j.energy.2017.01.067>.
- [105] C. Chen, L. Evans, A local composition model for the excess Gibbs energy of aqueous electrolyte systems, *AIChE J.* 32 (3) (1986) 444–454, <http://dx.doi.org/10.1002/aic.690320311>.
- [106] Y. Han, O. Oitoju, M. Wang, Renewable energy-driven solvent-based direct air capture and CO<sub>2</sub> utilisation to produce sustainable aviation fuel: Modelling, simulation and performance assessment, in: 17th International Conference on Greenhouse Gas Control Technologies, GHGT-17, 2024, pp. 1–8, <https://srm.com/abstract=5049793>.
- [107] M.M. Paulsen, S.B. Petersen, E.M. Lozano, T.H. Pedersen, Techno-economic study of integrated high-temperature direct air capture with hydrogen-based calcination and Fischer-Tropsch synthesis for jet fuel production, *Appl. Energy* 369 (2024) 123524, <http://dx.doi.org/10.1016/j.apenergy.2024.123524>.
- [108] A. Meurer, J. Kern, Fischer-Tropsch synthesis as the key for decentralized sustainable kerosene production, *Energies* 14 (7) (2021) 1836, <http://dx.doi.org/10.3390/en14071836>.
- [109] P. Wang, Q. Zhang, Economic analysis of syngas production by coupling coal gasification wastewater treatment and solid oxide cell system, *Chem. Eng. Trans.* 81 (2020) 1129–1134, <http://dx.doi.org/10.3303/CET2081189>.
- [110] K. Möller, P. Le Grange, C. Accolla, A two-phase reactor model for the hydrocracking of Fischer-Tropsch-derived wax, *Ind. Eng. Chem. Res.* 48 (2009) 3791–3801, <http://dx.doi.org/10.1021/ie801350p>.
- [111] Y. Han, A.D.N. Kamkeng, O. Oitoju, Y. Ding, M. Wang, Techno-economic assessment of modified Fischer-Tropsch to synthesis process for direct CO<sub>2</sub> conversion into jet fuel, *Fuel* 381 (2025) 133442, <http://dx.doi.org/10.1016/j.fuel.2024.133442>.
- [112] K. An, A. Farooqui, S.T. McCoy, The impact of climate on solvent-based direct air capture systems, *Appl. Energy* 325 (2022) 119895, <http://dx.doi.org/10.1016/j.apenergy.2022.119895>.
- [113] G. Holmes, D.W. Keith, An air-liquid contactor for large-scale capture of CO<sub>2</sub> from air, *Philos. Trans. R. Soc. A: Math. Phys. Eng. Sci.* 370 (2012) 4380–4403, <http://dx.doi.org/10.1098/rsta.2012.0137>.
- [114] M. Mostafa, C. Antonicelli, C. Varela, D. Barletta, E. Zondervan, Capturing CO<sub>2</sub> from the atmosphere: Design and analysis of a large-scale DAC facility, *Carbon Capture Sci. Technol.* 4 (2022) 100060, <http://dx.doi.org/10.1016/j.ccst.2022.100060>.
- [115] R. Singla, K. Chowdhury, Saving power by modifying a double column air separation plant to produce high and low purity pressurized gaseous oxygen simultaneously, *Energy* 210 (2020) 118487, <http://dx.doi.org/10.1016/j.energy.2020.118487>.
- [116] C. Fu, T. Gundersen, Using exergy analysis to reduce power consumption in air separation units for oxy-combustion processes, *Energy* 44 (2012) 60–68, <http://dx.doi.org/10.1016/j.energy.2012.01.065>.
- [117] A.D.N. Kamkeng, M. Wang, Long-term performance prediction of solid oxide electrolysis cell (SOEC) for CO<sub>2</sub>/H<sub>2</sub>O co-electrolysis considering structural degradation through modelling and simulation, *Chem. Eng. J.* 429 (2022) 132158, <http://dx.doi.org/10.1016/j.cej.2021.132158>.
- [118] F. Pattnaik, B.R. Patra, J.A. Okolie, S. Nanda, A.K. Dalai, S. Naik, A review of thermocatalytic conversion of biogenic wastes into crude biofuels and biochemical precursors, *Fuel* 320 (2022) 123857, <http://dx.doi.org/10.1016/j.fuel.2022.123857>.
- [119] International Energy Agency (IEA), *Energy statistics data browser*, 2022, URL: <https://www.iea.org/data-and-statistics/data-tools/energy-statistics-data-browser>. (Accessed 27 October 2025).
- [120] IDEA, *LCI Database Inventory Database for Environmental Analysis: IDEA, version 3*, Research Laboratory for IDEA/AIST Foundation, Sustainable Management Promotion Organization (SuMPO), 2025, <https://idea-ica.com/>. (Accessed 27 October 2025).
- [121] J.G. Speight, *The Chemistry and Technology of Petroleum*, fifth ed., CRC Press, 2014, <http://dx.doi.org/10.1201/b16559>.
- [122] M. Bui, C.S. Adjiman, A. Bardow, E.J. Anthony, A. Boston, S. Brown, P.S. Fennell, S. Fuss, A. Galindo, L.A. Hackett, et al., Carbon capture and storage (CCS): the way forward, *Energy Environ. Sci.* 11 (5) (2018) 1062–1176, <http://dx.doi.org/10.1039/C7EE02342A>.
- [123] U.K. Department for Environment, Food & Rural Affairs, *Greenhouse gas reporting conversion factors 2025*, 2025, URL: <https://www.gov.uk/government/publications/greenhouse-gas-reporting-conversion-factors-2025>. (Accessed 19 December 2025).
- [124] GlobalPetrolPrices.com, *Electricity prices*, 2022, URL: [https://www.globalpetrolprices.com/electricity\\_prices/](https://www.globalpetrolprices.com/electricity_prices/). Prices of September 2021.
- [125] International Renewable Energy Agency (IRENA), *Renewable Power Generation Costs in 2020, 2021*, URL: <https://www.irena.org/Statistics/View-Data-by-Topic/Costs/Global-Trends>.
- [126] GlobalPetrolPrices.com, *Methane prices*, 2022, URL: [https://www.globalpetrolprices.com/methane\\_prices/](https://www.globalpetrolprices.com/methane_prices/). Industrial fuel price data.
- [127] K.J. Jabbar, S.H. Zein, A.H. Hasan, U. Ahmed, A.A. Jalil, Process design optimisation, heat integration, and techno-economic analysis of oil refinery: A case study, *Energy Sources Part A: Recover. Util. Environ. Eff.* 45 (2) (2023) 4931–4947, <http://dx.doi.org/10.1080/15567036.2023.2205365>.
- [128] J. Gary, G. Handwerk, *Petroleum Refining: Technology and Economics*, fifth ed., CRC Press, 2007.
- [129] N.W.R.S. Refinery, What are the numbers for Alberta's investment? *Sustain. Prosper. Policy Pap.* (2018) URL: <https://journalhosting.ucalgary.ca/index.php/sppp/article/view/53039>.